JOURNAL OF PETROLOGY | VOLUME 41 | NUMBER 2 | PAGES 201–227 | 2000

Late Devonian Diamondiferous Kimberlite and Alkaline Picrite (Proto-kimberlite?) Magmatism in the Arkhangelsk Region, NW Russia

I. L. MAHOTKIN[1], S. A. GIBSON[2]*, R. N. THOMPSON[3], D. Z. ZHURAVLEV[4] AND P. U. ZHERDEV[5]

[1]DE BEERS CENTENARY (RUSSIA), UL. TVERSKAYA 22A, MOSCOW, 103050, RUSSIA

[2]DEPARTMENT OF EARTH SCIENCES, UNIVERSITY OF CAMBRIDGE, DOWNING STREET, CAMBRIDGE CB2 3EQ, UK

[3]DEPARTMENT OF GEOLOGICAL SCIENCES, UNIVERSITY OF DURHAM, SOUTH ROAD, DURHAM DH1 3LE, UK

[4]INSTITUTE OF ORE DEPOSITS (IGEM), RUSSIAN ACADEMY OF SCIENCES, STAROMONETNY 35, MOSCOW 109017, RUSSIA

[5]GEOLOGICAL ENTERPRISE 'ARKHANGELSK GEOLOGY', TROITSKY PROSPECT 137, ARKHANGELSK, 163001, RUSSIA

RECEIVED MARCH 1, 1999; REVISED TYPESCRIPT ACCEPTED JULY 14, 1999

Widespread penecontemporaneous igneous activity affected NW Russia (the Kola Peninsula and adjoining areas to the SE around Arkhangelsk) during the Late Devonian (360–380 Ma). Magmatism varies from tholeiitic basalts, erupted in the axial regions of former Middle Proterozoic (Riphean) rifts, to strongly alkaline rock-types on and marginal to Archaean cratons. NNE of Arkhangelsk kimberlites, olivine lamproites and alkaline picrites were emplaced; all these rock-types are diamondiferous to varying extents. Higher TiO_2 (and also total Fe) distinguish predominantly mica-poor Eastern Group kimberlites (TiO_2 = 2·4–3·1 wt %) and spatially associated alkaline picrites (TiO_2 = 3·2–3·7 wt %) from nearby micaceous Western Group kimberlites (TiO_2 = 0·8–1·1 wt %). Each rock-type also has distinctive rare earth element (REE) patterns, and εNd ranges: micaceous kimberlites, $(La/Yb)_n$ = 19·1–44·4, εNd = −2·4 to −3·6; olivine lamproites, $(La/Yb)_n$ = 76·9, εNd = −4·6 to −4·7; mica-poor kimberlites, $(La/Yb)_n$ = 86·3–128·2, εNd = 0·0–2·5; alkaline picrites, $(La/Yb)_n$ = 13·1–17·9, εNd = 0·1–1·1. Variations in the petrography and bulk-rock chemistry of the Arkhangelsk kimberlites are superficially similar to South African Group I and II kimberlites. Despite their field proximity, the alkaline picrite REE patterns contrast with those of the kimberlites. Instead, they closely resemble those of 'protokimberlites', the hypothetical magmas calculated to have precipitated South African kimberlite subcalcic clinopyroxene, garnet and ilmenite megacrysts at base-of-lithosphere depths (~200 km). Our new data, combined with published studies of Arkhangelsk kimberlites and the silicate inclusions in their diamonds, support a genetic model where protokimberlite magmas separated from sub-lithospheric convecting mantle at several hundreds of kilometres depth. During their uprise through ~200 km thick lithosphere, some magma batches dissolved predominantly ilmenite on a minor scale and erupted as mica-poor alkaline picrites and kimberlites. Others reacted wholesale with fusible lithospheric components to produce micaceous alkaline picrites and diamondiferous kimberlites.

KEY WORDS: *kimberlite; protokimberlite; alkaline picrite; Kola craton; diamondiferous*

INTRODUCTION

In both the oceanic and continental environments, it is clear that variations in the 'local' (scale comparable with

*Corresponding author. Telephone: +44-1223 333400. Fax: +44-1223 333450. e-mail: sally@esc.cam.ac.uk

that of the 2000 km diameter plume head) lithospheric thickness will strongly influence the presence, abundance and composition of plume-related magmatism (e.g. Thompson & Gibson, 1991; Sleep, 1996, 1997). This is because of the sensitivity of both the amount and composition of decompression melts to lithospheric thickness (e.g. White & McKenzie, 1995). Where the lithosphere is thick, the magmatism may (1) be relatively small in volume, and (2) include strongly alkaline rock-types, such as kimberlites, lamproites, nephelinites and melilitites. The highly enriched trace element concentrations of many mafic alkaline igneous rocks require that their contributing parental melts were derived (at least in part) from a metasomatized lithospheric mantle source (e.g. McKenzie, 1989; Gibson *et al.*, 1993, 1995*a*, 1995*b*; Thompson *et al.*, 1998).

Tainton & McKenzie (1994) have proposed that the REE patterns of kimberlites and lamproites require a two-stage mantle melting model. They envisaged a lithospheric mantle source, initially depleted by melt extraction and then subsequently enriched in trace elements, before kimberlite genesis. Such models are closely related, in their outcome, to those that postulate that kimberlites begin as melts within the convecting mantle, beneath the lithosphere, and then react with and dissolve lithospheric debris during their uprise (e.g. Haggerty, 1994; Pearson *et al.*, 1995; Nowell & Pearson, 1998). The REE modelling of Tainton & McKenzie (1994) deduced that the kimberlite component derived from convecting mantle (their precursor small-fraction metasomatizing melts) were extracted from depleted upper mantle; the same reservoir as mid-ocean ridge basalt (MORB). Harte (1983) and Jones (1987) approached this matter differently, by analysing the trace elements and Sr–Nd isotopic ratios of the clinopyroxene and garnet megacrysts that occur in some South African kimberlites. They showed that these were not in chemical equilibrium with the kimberlites that contained them. Instead, the megacrysts appeared to have precipitated from alkalic picritic ('proto-kimberlite') melts that resembled oceanic alkali–olivine basalts and basanites geochemically and appear to have originated from a primitive rather than a depleted convecting mantle source.

This study is concerned with the Late Devonian Arkhangelsk Alkaline Igneous Province (AAIP), which is itself a subset of widespread penecontemporaneous basaltic to strongly alkaline magmatism in NE Europe (Fig. 1). This igneous activity is believed to have been caused by the sub-lithospheric impact of a Late Devonian mantle plume (Mahotkin *et al.*, 1995, 1997; Parsadanyan *et al.*, 1996; Beard *et al.*, 1998; Marty *et al.*, 1998). The AAIP is situated in the northeast of the East European Platform (Fig. 1) and comprises a wide variety of ultramafic alkaline rock-types, including kimberlites, with a rare olivine lamproite variant, and alkaline picrites. In the middle 1970s richly diamondiferous kimberlite pipes were discovered in the region (Stankovskiy *et al.*, 1977; Stankovskiy *et al.*, 1979) and such discoveries have continued (Verichev *et al.*, 1998). Significantly, some of the alkaline picrites are also diamondiferous. These rocks lack kimberlite macrocrysts and xenoliths and are characterized by pseudomorphs that appear to be after melilitite. We shall suggest that the alkaline picrites resemble geochemically the hypothetical 'proto-kimberlite' that has been proposed in previous studies of South African kimberlites (Harte, 1983; Jones, 1987).

GEOLOGY OF THE ARKHANGELSK REGION

The tectonic structure, age and composition of the basement beneath the AAIP strongly influenced (1) the location of Late Devonian magmatic activity, (2) magma composition and (3) the extent to which it is diamondiferous (Sinitsin *et al.*, 1992; Sablukova *et al.*, 1995). We shall therefore review the Precambrian and Lower Palaeozoic tectonomagmatic evolution of the Arkhangelsk region before discussing the Devonian magmatism.

Precambrian tectonomagmatic evolution of the Baltic Shield

The East European Platform, a collage of Archaean cratons and Early Proterozoic mobile belts, underlies most of western Russia and the Baltic states. Riphean to Palaeozoic sediments cover most of the platform to the south and east of Scandinavia (Blundell *et al.*, 1992). The Baltic Shield, the NW segment of the platform, has been investigated in considerable detail (e.g. Khain & Bozhko, 1988; Nikishin *et al.*, 1996). In its eastern part there are two Archaean cratons, Kola and Karelia, separated by the Early Proterozoic Belomorian mobile belt (Fig. 1). The cratons are composed of Early Archaean tonalitic gneisses and granulites, surrounded by narrow greenstone belts, containing both sedimentary and volcanic rocks. These units were reworked in the Belomorian belt, with accompanying amphibolite-facies metamorphism, granite emplacement and crustal thickening. The southeastward extensions of both cratons and the Belomorian belt are hidden beneath a Riphean–Palaeozoic sedimentary cover, in the Arkhangelsk area (Fig. 1).

Subsequent development of the Baltic Shield involved the formation of the Middle Proterozoic (Riphean) Kola–Belomorian graben system, an offshoot of the rift system that affected the entire East European Platform (Bogdanova *et al.*, 1996). This extension was crucially

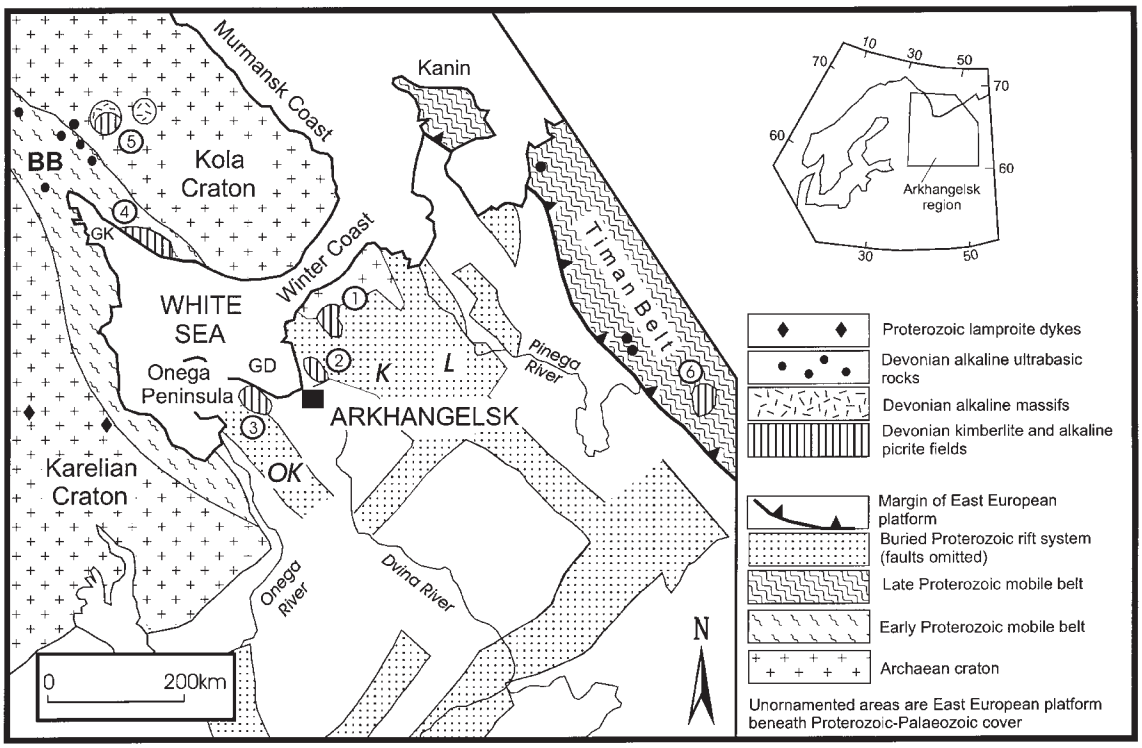

Fig. 1. Tectonic setting of the Arkhangelsk Alkaline Igneous Province (AAIP) and other parts of the Late Devonian Kola Alkaline Igneous Province (Konstantinovskiy, 1977; Khain & Bozhko, 1988; Kogarko *et al.*, 1995). BB, Belomorian mobile belt; OK, Onega–Kandalaksha rift; K, Keretskiy rift; L, Leshukonskiy rift; GK, Gulf of Kandalaksha; GD, Gulf of Dvina. Alkaline volcanic fields: 1, Zimniy Bereg (comprising Zolotitsa, Verkhotina–Soyana and Kepino–Pachuga); 2, Chidvia–Izhmozero; 3, Nenonksa; 4, Terskii Coast; 5, Khibiny; 6, Middle Timan. It should be noted that the extensive Riphean–Palaeozoic sedimentary cover and the offshore extensions of the rifts, under the White and Barents Seas, have been omitted for clarity.

important in controlling both the siting and nature of the subsequent Devonian alkaline magmatism; it fragmented the uniformly thick lithosphere of the Baltic Shield in the Kola–Arkhangelsk area into blocks where the lithosphere remained thick, separated by a network of Middle Proterozoic rifts (Fig. 1) where the lithosphere was significantly thinner. In general, the Middle Proterozoic rifts were sited within the Belomorian and other Early Proterozoic former mobile belts but a few (e.g. Leshukonskiy) affected the margins of the cratons. One well-studied graben, Onega–Kandalaksha, provides important information about these rifts in general (Konstantinovskiy, 1977; Salop, 1982; Khain & Bozhko, 1988; Shcheglov *et al.*, 1993). It extends NW–SE from Finland through the head of the Gulf of Kandalaksha to the Onega Peninsula (Fig. 1). Its red-bed dominated sedimentary infilling also includes tholeiitic basalts and ferrobasalts (K–Ar age 1300 Ma; Staritskiy, 1981; Sinitsin *et al.*, 1982). Later Vendian sediments complete the infilling and overlap the graben shoulders. Further Riphean tholeiitic basalt dykes and sills cut the NE margin of the Kola craton, adjacent to another Riphean graben (Staritskiy, 1981; Berkovsky & Platunova, 1989). Within the Kola and Karelia cratons, Riphean magmatism is represented by lamproitic dykes (Proskuriykov *et al.*, 1992), as shown in Fig. 1. Some of these have been recently reclassified as kimberlites (Mahotkin, 1998).

The ~1300 Ma tholeiitic basalts are useful in reconstructing the pre-Devonian tectonic framework of the Arkhangelsk–Kola region. Enough is now known about the interrelationships between lithospheric plate thickness, mantle potential temperature and the compositions of basaltic (*sensu lato*) melts (e.g. McKenzie & Bickle, 1988; White & McKenzie, 1995) to be able to deduce that total lithospheric thickness was reduced by extension to <100 km beneath the Riphean rifts. In a region that has lacked subsequent major compressional tectonic episodes, the thinned lithosphere zones could only have rethickened conductively to ~125 km (McKenzie, 1989), a value about half that to be expected (200 km or more; McKenzie, 1989; Pearson, 2000) beneath undisturbed Archaean cratons.

Late Devonian magmatic activity in NW Russia

A short intense, widespread phase of Late Devonian (~380–360 Ma) mafic, alkaline-ultramafic and carbonatitic magmatism immediately followed large-scale lithospheric doming of the East European Platform (Staritskiy, 1981; Sablukov, 1984; Kramm *et al.*, 1993; Zaitsev & Bell, 1995; Beard *et al.*, 1996, 1998; Nikishin *et al.*, 1996; Wilson & Lyashkevich, 1996). In the Kola–Arkhangelsk–Timan area (Fig. 1), it was associated with further localized doming, centred on the Kola Peninsula (Nikishin *et al.*, 1996). The style of magmatism varied from the eruption of tholeiitic basalts to the emplacement of large alkaline igneous complexes and relatively small-volume ultramafic alkaline pipes and sills.

Tholeiitic basalts

Late Devonian (Frasnian) tholeiitic lavas and tuffs form a 300 m thick volcano-sedimentary succession (Staritskiy, 1981) that outcrops over an area of 2500 km^2 and extends from the Kanin Peninsula to Middle Timan. Outlying tholeiitic plugs of the province are marked in Fig. 2 (Mahotkin *et al.*, 1995; Parsadanyan *et al.*, 1996). Other occurrences of Late Devonian magmatism are found throughout the Timan–Pechora region and along the Murmansk coast of the Kola Peninsula (Staritskiy, 1981; Ishmail-Zadeh *et al.*, 1997). These extensive tholeiitic lavas, referred to as the Timan–Kola flood-basalts by Sinitsin & Kushev (1968), are associated with a major tholeiitic dyke swarm (Berkovsky & Platunova, 1989) that extends ~2500 km N–S and links Late Devonian magmatism throughout the East European Platform into a single igneous megaprovince (Wilson & Lyashkevich, 1996).

Alkaline-ultramafic igneous complexes

The Late Devonian magmatism of the Kola region forms one of the world's largest intrusive and sub-volcanic alkaline provinces. The Kola Alkaline Province outcrops over an area of ~100 000 km^2 and comprises 24 igneous complexes (Dudkin & Mitrofanov, 1993; Kogarko *et al.*, 1995). Most of these were intruded during a very short time interval (380–360 Ma) in the Late Devonian (Kramm *et al.*, 1993; Beard *et al.*, 1996, 1998). There are three types: (1) nepheline syenite complexes, e.g. Khibina and Lovozero (Kogarko *et al.*, 1995); (2) alkaline-ultramafic complexes predominantly composed of peridotites, pyroxenites and ijolites, e.g. Kovdor (Zaitsev & Bell, 1995) and Afrikanda; (3) complexes containing significant carbonatite, e.g. Sokli (Vartiainen & Paarma, 1979) and Telyachi Island (Beard *et al.*, 1996). The largest alkaline intrusive complexes were emplaced in the Kontozero graben, Kola Peninsula. Lithospheric extension and sedimentation associated with this major NW-trending rift zone began at ~375 Ma (Nikishin *et al.*, 1996). The relatively small-volume carbonatite bearing complexes have a more scattered distribution across the Kola craton (Kramm *et al.*, 1993). Outside the Arkhangelsk area kimberlite diatremes and dykes of kimberlite-like rock-types are known from the Terskii Coast field (Beard *et al.*, 1998; Fig. 1).

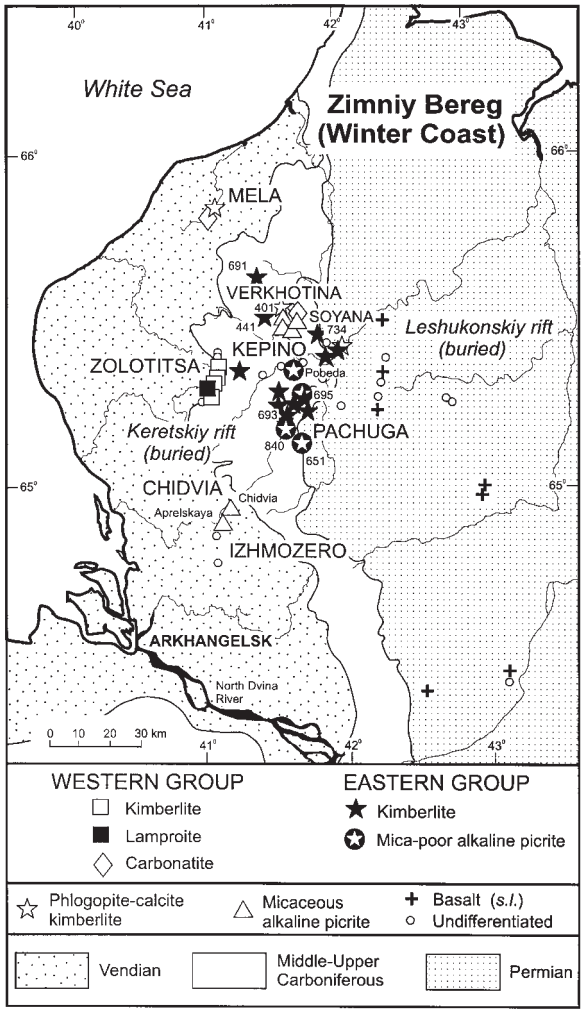

Fig. 2. Simplified geological sketch map of the AAIP, showing the locations of diatremes, etc. discussed in the text. Sedimentary geology after Sinitsin & Grib (1995).

THE ARKHANGELSK ALKALINE IGNEOUS PROVINCE (AAIP)

The small-volume Arkhangelsk igneous activity is mostly in the form of sub-volcanic pipes (diatremes), together with some sills (Sinitsin & Grib, 1995). Clusters of diatremes form several igneous fields (Fig. 2), each with distinctive petrological characteristics. The fields occur

in two groups on the SE side of the White Sea: (1) along and up to 100 km inland from the Zimniy Bereg (i.e. Winter Coast); (2) on the NE side of the Onega Peninsula, separated from the Zimniy Bereg by the Gulf of Dvina (Fig. 1). Table 1 summarizes various features of the AAIP localities discussed in this paper. Although our study is far from comprehensive, the samples come from all the main AAIP igneous fields north of Arkhangelsk and include most of the better-known diamondiferous diatremes (e.g. Sinitsin & Grib, 1995; Parsadanyan *et al.*, 1996). Others have been discussed by Mahotkin *et al.* (1995, 1997).

A zone of normal faults with NE–SW trends extends throughout the AAIP. These are not shown in Fig. 2 because, like the Riphean grabens, they are mostly buried beneath Upper Palaeozoic sediments. Both limited crustal thinning and remnants of Upper Devonian to Lower Carboniferous sediments preserved along this zone are considered to be evidence for weak Devonian extension (Grib *et al.*, 1987; Nikishin *et al.*, 1996). Most of the AAIP diatremes are thought to be sited at the intersection of NE–SW faults and the shoulders of former Riphean grabens. Specifically: (1) the Chidvia–Izhmozero alkaline picrites and other rock-types (Table 1) are emplaced at the SW margin of the Keretskiy graben (Fig. 1); (2) most of the kimberlites, lamproites and alkaline picrites of the other Zimniy Bereg fields (Zolotitsa, Mela, Kepino–Pachuga and Verkhotina–Soyana; Table 1) are emplaced in Vendian sediments (Erinchek *et al.*, 1998) that are believed to cover the NE margin of the Keretskiy graben, the west margin of the Leshukonskiy graben and its Padun extension (Fig. 1), and adjacent Archaean Kola cratonic basement—the Ruch'y and Zolotitsa horsts (Sinitsin & Grib, 1995).

Field characteristics of the igneous rocks

The diamondiferous-kimberlite diatremes of the Zolotitsa cluster and the alkaline picrite pipe at Chidvia are typical examples of the Zimniy Bereg pipes. Figure 3 shows a plan and sections of one of these, Pionerskaya (Table 1). Information about these diatremes comes from drillcore samples. The vent deposits consist of either one or two phases of breccia. The first phase comprises diverse polylithic tuffs and breccias, which are often layered and consist of rounded fragments (lapilli) of kimberlites or alkaline picrites, olivine pseudomorphs, xenoliths of country rocks and quartz sand (Sablukov, 1987). The fragments are present in various proportions, giving a range of clastic rock-types from autolithic tuffs to sandstones and sedimentary breccias. Clast sizes in igneous breccias are notoriously difficult to estimate in drillcores. The smallest clasts are encompassed by thin sections (e.g. Fig. 4b) but it is not easy to be sure whether the largest igneous samples are from clasts or later dykes. Subhorizontal microlamination, fragment size-sorting, plant remains (Lower Frasnian) and xenoliths of Early and Middle Palaeozoic sedimentary rocks can be traced down to a depth of 600 m (Sablukov, 1987). The polylithic tuffs and breccias are intruded by kimberlite (or alkaline picrite) breccia that consists of lapilli and altered olivines, cemented by a serpentine–saponite mixture, with additional minor talc, richteritic amphibole and diverse carbonates. The relative volumes of polylithic and autolithic igneous breccias vary amongst the different pipes and within each one.

Most of the diatremes have well-developed infilled craters that appear to have undergone little erosion. These are trough-like or saucer-shaped and are infilled by flat-lying tuffs and interbedded tuffaceous sediments, sandstones and sedimentary breccias. There are also zones of cross-laminated, fine-grained accretionary lapilli tuff (Sablukov, 1987). In addition to the main pipes, several 0·5–3 m thick sills of kimberlite, with local carbonate facies, are exposed within Vendian arenites along the River Mela. These closely resemble the Benfontein Sill, South Africa (Dawson & Hawthorne, 1973).

PETROGRAPHY AND MINERALOGY

Approximately 1200 samples have been collected from the hypabyssal and diatreme crater facies of the pipes in the AAIP together with the Mela sills. Table 1 summarizes the rock-types encountered. They can be classified into two groups: (1) kimberlites (Woolley *et al.*, 1996), with minor olivine lamproites and carbonatites; (2) alkaline picrites. Sablukova (1995), Sablukova *et al.* (1995) and Sobolev *et al.* (1997) have given recent accounts of their included xenoliths and macrocrysts.

Kimberlites

Kimberlites are the predominant rock-type in the Zolotitsa and Mela fields, and a component of the Kepino–Pachuga and Verkhotina–Soyana fields. They can be divided geographically (Fig. 2) into a predominantly mica-poor Eastern Group and a predominantly micaceous Western Group, superficially similar to Group I and Group II South African kimberlites, respectively (Parsadanyan *et al.*, 1996). Nevertheless, as emphasized in the previous section, the AAIP kimberlites are mostly fragmented and hence drastically affected by post-magmatic alteration. Only the Pionerskaya pipe has yielded a massive facies. This occurs in a drill-hole (1490; Fig. 3); between 850 and 1000 m there are several 10–30 m massive kimberlite units amongst the breccias. They may be either exceptionally large clasts or post-breccia dykes.

Table 1: Igneous rocks of the Arkhangelsk province discussed in this paper

Igneous field	Locality	Intrusive form	Rock-type	Diamonds? 0 = none	Analysed for:	Mineralogy: Probably magmatic	Mineralogy: Probably hydrothermal
Western Group							
Zolotitsa	Pionerskaya	Pipe	Kimberlite	2	Elements + isotopes	mol, pol, gol, phlog, glog, pv, (mont), amph, cpx, sp	serp, sap, hgr, pect, cal
	Lomonosovskaya	Pipe	Kimberlite	3	Elements + isotopes	mol, pol, gol, glog, (mont), pv	serp, sap, cal
	Karpinskiy II	Pipe	Kimberlite	2 to 3	Elements + isotopes	mol, pol, phlog, glog, (mel), cpx, amph, pv	serp, sap, hgr
	Karpinskiy I	Pipe	Kimberlite	2 to 3	Elements + isotopes	(mol), (pol), (gol), phlog, glog, amph	sap, hgr, talc, cal, seric
	Karpinskiy I	Pipe	Olivine lamproite	2 to 3	Elements + isotopes	mol, pol, glog, amph, cpx	sap, seric
	Arkhangelskaya	Pipe	Kimberlite	3	Elements	(mol), (pol), (gol), phlog, glog, amph	sap, hgr, chlor, talc, cal, seric
Mela	Mela I	Sill	Kimberlite	0	Elements + isotopes	(pol), phlog, cal, pv, sp	serp, sap, cal, chlor
	Mela I and III	Sills	Carbonatite	0	Elements + isotopes	cal, apatite, phlog	serp, chlor
Eastern Group							
Verkhotina–Soyana	Anomaly 401	Pipe	Alkaline picrite	1	Isotopes	(pol), (ol), (mel), cpx, glog, pv, sp	sap, hgr, cal
	Anomaly 401	Pipe	Kimberlite	1	Isotopes	pol, phlog, cal, apatite	serp, sap, hgr
	Anomalies 691, 734	Pipes	Kimberlite	1	Isotopes	mol, pol, gol, phlog, glog, (mont), pv, sp,	serp, sap, chlor, cal, hgr
Kepino–Pachuga	Anomaly 688	Pipe	Kimberlite	2	Isotopes	mol, pol, gol, phlog, glog, pv, sp, (± mont)	serp, sap, chlor, cal, hgr
	Anomaly 693	Pipe	Kimberlite	1	Elements + isotopes	mol, pol, gol, phlog, glog, (mont), pv, sp,	serp, sap, cal, hgr
	Anomaly 695	Pipe	Kimberlite	1	Elements + isotopes	pol, gol, glog, (mont), pv, sp	serp, hgr
	Anomalies 651, 840	Pipes	Alkaline picrite	1	Elements + isotopes	(pol), (gol), (mel), sp	serp, sap, hgr, cal
	Pobeda	Pipe	Alkaline picrite	0	Isotopes	(pol), (gol), (mel), sp	serp, sap, hgr, cal
Chidvia–Izhmozero	Chidvia	Pipe	Alkaline picrite	1	Elements + isotopes	(mol), (pol), (gol), phlog, glog, (mel), cpx, sp	sap, hgr (+ quartz xenocrysts)
	Aprelskaya	Pipe	Alkaline picrite	1	Elements + isotopes	pol, (mel), glog, cpx, cal, pv, sp	sap, cal

Place-names are anglicized to versions judged most pronouncible by international readers; they follow British Standard 2979, with the modifications of Kogarko *et al.* (1995). Most pipe samples are breccia blocks (autoliths). Their mineralogy therefore refers to more than one block in many cases. Mineral abbreviations: mol, macrocryst olivine; pcpx, phenocryst clinopyroxene; mont, monticellite; hgr, hydroandradite; pol, phenocryst olivine; cpx, groundmass clinopyroxene; pv, perovskite; pect, pectolite; gol, groundmass olivine; amph, richteritic amphibole; sp, spinel; cal, calcite; phlog, phenocryst phlogopite; mel, melilite; serp, serpentine; chlor, chlorite; glog, groundmass phlogopite; ne, nepheline; sap, saponite; seric, sericite; ( ), completely pseudomorphed mineral. Scale for diamonds: 0, diamond-free; 3, richly diamondiferous. Anomaly 441 (Grib Pipe), marked in Fig. 2 but not discussed in this paper, also classifies as 3 (Verichev *et al.*, 1998).

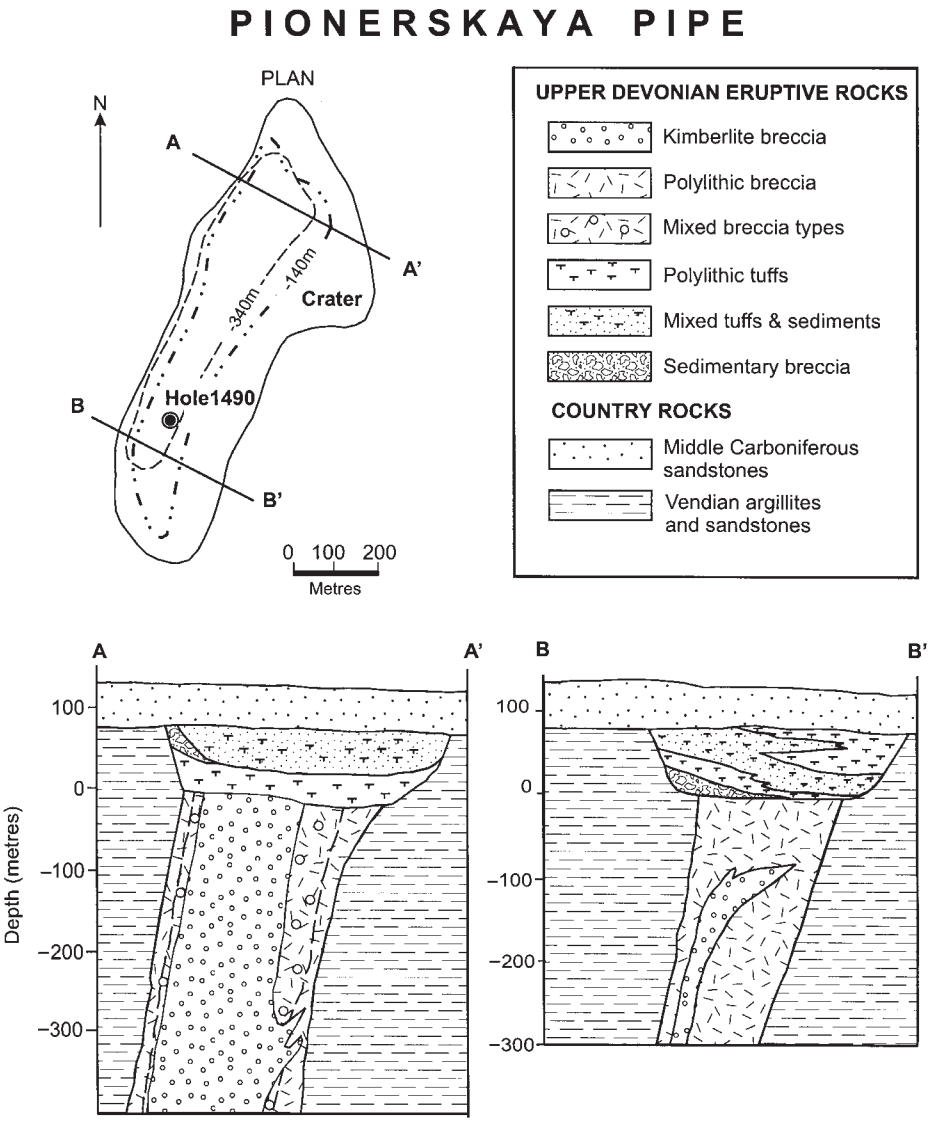

Fig. 3. Plan and sections of the Pionerskaya pipe, Zolotitsa field.

Western Group kimberlites

Kimberlites in the Western Group are predominantly micaceous (Table 1). Most of the richly diamondiferous diatremes are formed by this rock-type. The freshest samples come from the massive facies of the Pionerskaya pipe. They consist principally of macrocrysts and phenocrysts of fresh olivine, together with microphenocrysts of phlogopite. Subhedral to anhedral olivine macrocrysts range from 2 to 12 mm and form 25–30 modal % of the rock. The macrocrysts have high *mg*-numbers (92·3–92·6) and Ni contents, and low Ca contents (Table 2), thus resembling olivine macrocrysts from the Udachnaya kimberlite, Yakutia (Sobolev *et al.*, 1989), and olivine inclusions in diamonds (Hervig *et al.*, 1980). Euhedral olivine phenocrysts (0·01–1·2 mm in length) form up to 25% of the rock. They have less-magnesian core compositions (*mg*-number = 89·9–90·6) and are depleted in Ni and enriched in Ca, relative to the olivine macrocrysts (Table 2). They are zoned, with *mg*-number increasing and Ni decreasing outwards (Table 2). The smallest crystals are partly or totally altered to serpentine and saponite.

The modal abundance of phlogopite varies from 15 to 35% of the rock, but in exceptional cases it may constitute up to 60%. Sparse magnesian phlogopite microphenocrysts (up to 0·3 mm), with *mg*-number 92–93 and low Ti contents (Tables 3 and 4), surround the olivine grains. Phlogopite also occurs as <1·5 mm poikilitic anhedral plates that enclose olivine phenocrysts,

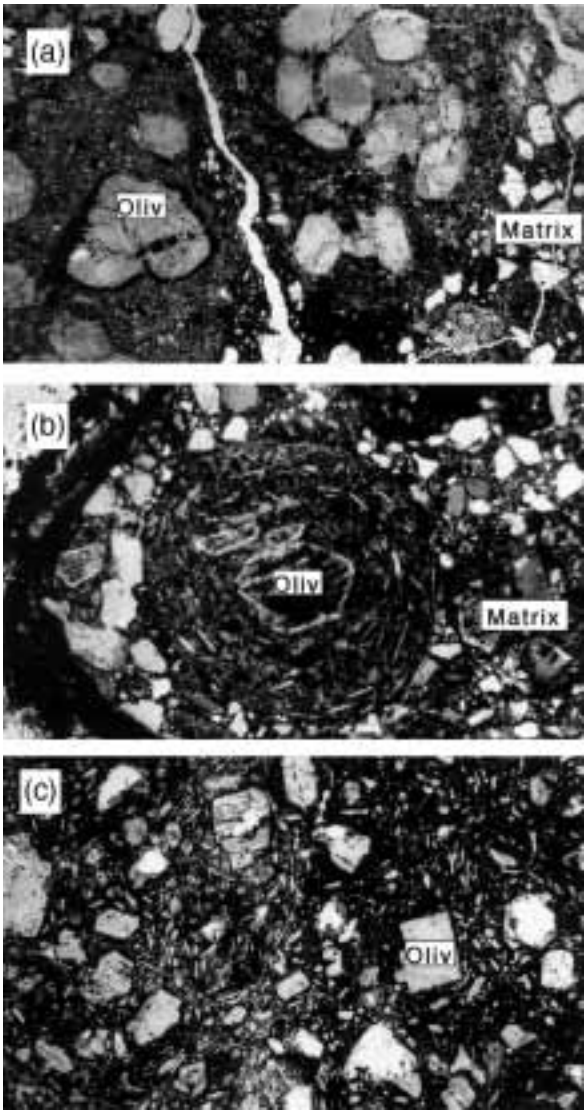

Fig. 4. Photomicrographs (plane-polarized light) of alkaline picrite clasts in Arkhangelsk diatreme breccias. (See Table 1 for summary of mineralogy.) Field of view is 6 mm wide in each case. (a) Part of a picrite clast, with euhedral–subhedral pseudomorphed olivine phenocrysts in a groundmass of secondary minerals. The surrounding breccia matrix contains both igneous and sedimentary grains (Anomaly 651 pipe; 711/210). (b) Another Anomaly 651 clast (711/100), showing euhedral pseudomorphed olivine phenocrysts surrounded by tangentially arranged elongate pseudomorphs after supposed melilite (see text for discussion). This clast appears to be a pelletal lapillus (Mitchell, 1986). (c) Another clast, showing abundant pseudomorphed groundmass, supposed melilite, plus fresh phlogopite, surrounding euhedral–subhedral pseudomorphed olivine phenocrysts (Chidvia pipe; 752/66).

Table 2: Representative analyses of olivines from the Pionerskaya pipe (1490/1017)

	Macrocryst			Phenocryst		Micro-phenocryst
	core	core	rim	core	rim	
wt %						
SiO_2	41·10	41·14	41·60	41·25	41·75	40·89
FeO	7·58	7·46	7·21	9·06	8·11	9·79
MnO	b.d.	0·18	b.d.	0·15	0·16	b.d.
MgO	50·18	50·79	50·69	49·02	49·92	48·86
CaO	0·03	0·03	0·04	0·06	0·10	0·06
NiO	0·37	0·36	0·34	0·28	0·26	0·30
Total	99·56	99·87	99·88	99·82	100·14	99·90
Mg/(Mg+Fe)	0·922	0·924	0·926	0·906	0·916	0·899

b.d., below detection limit.

Table 3: Representative analyses of micas from the Pionerskaya pipe (1490/1017)

	mphen	gdm	gdm	gdm	gdm	gdm	gdm
wt %							
SiO_2	42·71	41·20	39·24	39·74	40·05	40·99	40·10
TiO_2	0·62	0·67	0·05	1·26	0·17	1·62	1·12
Al_2O_3	12·29	10·53	12·07	9·20	10·90	7·40	9·87
FeO	2·43	4·53	11·43	7·06	9·82	9·25	9·04
MnO	b.d.	b.d.	0·19	b.d.	0·48	0·15	b.d.
MgO	24·94	26·38	21·52	26·29	23·28	24·54	24·18
CaO	0·04	0·34	0·38	0·14	0·26	0·14	1·14
K_2O	9·25	9·71	8·47	9·22	9·31	10·08	9·07
Cr_2O_3	0·56	b.d.	b.d.	b.d.	b.d.	b.d.	0·16
Total	92·84	93·35	93·30	92·91	94·17	94·17	94·68
Mg/(Mg+Fe)	0·948	0·912	0·770	0·869	0·809	0·825	0·827

mphen, microphenocryst; gdm, poikilitic plates in groundmass; b.d., below detection limit.

perovskite (Table 5) and small crystals of a phase that has been entirely replaced by pectolite and hydroandradite (Table 5). The groundmass phlogopite crystals vary in *mg*-number from 91·2 to 77 (Tables 3 and 4). Figure 5 is a plot of TiO_2 and Al_2O_3 in AAIP phlogopites, showing their relationship to micas from other kimberlites, mafic ultrapotassic rock-types and mantle xenoliths. This diagram includes microphenocryst phlogopite from the kimberlite clasts of the Arkhangelskaya pipe (Table 4), which illustrate the extensive compositional range of the AAIP kimberlite micas (Parsadanyan *et al.*, 1996).

A mineral that resembles an alkaline amphibole is present as extremely small crystals in the groundmass (Table 5). Its analysis has relatively high CaO, which

Table 4: Representative analyses of mica from the Arkhangelskaya pipe

	Microphenocrysts									
wt %										
SiO_2	39·35	38·50	39·56	40·46	41·85	42·43	41·11	42·71	42·07	41·96
TiO_2	1·63	2·28	2·07	0·83	0·83	0·76	0·73	0·62	0·61	0·38
Al_2O_3	13·24	14·54	13·61	14·65	11·84	11·82	12·22	12·29	11·46	10·69
FeO	3·46	3·99	5·33	1·88	3·12	3·07	3·21	2·43	3·72	3·32
MnO	b.d.	b.d.	0·02	b.d.	b.d.	0·04	0·02	b.d.	0·03	0·07
MgO	23·29	22·33	21·79	23·84	25·42	25·10	24·85	24·94	24·73	25·31
CaO	0·02	0·02	b.d.	b.d.	b.d.	b.d.	0·02	0·04	b.d.	b.d.
K_2O	9·09	8·56	9·08	8·89	9·58	10·00	10·27	9·25	9·42	9·49
Cr_2O_3	1·71	0·71	0·14	0·46	0·42	0·31	0·43	0·5	0·32	0·57
Na_2O	0·32	0·52	0·28	0·69	0·04	0·18	0·21	0·06	0·22	0·19
Total	92·11	91·52	91·88	91·70	93·10	93·71	93·07	92·90	92·58	91·98
Mg/(Mg+Fe)	0·923	0·909	0·879	0·958	0·936	0·936	0·932	0·948	0·922	0·932

b.d., below detection limit

Table 5: Representative analyses of groundmass minerals from the Pionerskaya pipe (1490/1017)

	Perov	Pect	Hgr	Amph	Sap*	Sap
wt %						
SiO_2	3·60	49·02	26·78	45·65	32·81	41·79
TiO_2	50·80	0·30	2·66	0·21	b.d.	b.d.
Al_2O_3	0·68	0·43	2·58	4·63	7·52	1·27
FeO	2·02	1·60	21·38	5·59	3·77	6·57
MnO	0·29	b.d.	0·30	0·18	b.d.	0·17
MgO	2·07	b.d.	b.d.	14·11	37·56	35·18
CaO	36·10	34·03	34·56	16·69	0·14	0·15
Na_2O	0·72	7·51	0·56	4·75	0·33	b.d.
K_2O	0·94	0·12	b.d.	3·14	0·21	0·95
Cr_2O_3	0·41	0·22	b.d.	0·27	b.d.	b.d.
Cl	b.d.	b.d.	b.d.	0·07	0·55	0·07
Total	97·62	93·24	88·94	94·95	81·88	86·15

Perov, perovskite; Pect, pectolite; Hgr, hydrogarnet; Amph, alkaline amphibole; Sap, saponite (*sum includes 1·21 wt % SO_3). b.d., below detection limit.

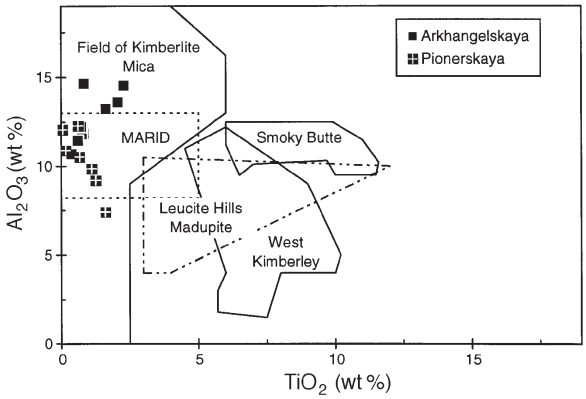

Fig. 5. Variation of TiO_2 and Al_2O_3 in phlogopite crystals from the Pionerskaya and Arkhangelskaya kimberlites (Tables 3 and 4). The fields of phlogopite in kimberlites, selected lamproites and the MARID (mica–amphibole–rutile–ilmenite–diopside) xenolith suite are shown for comparison (Dawson & Smith, 1977; Smith *et al.*, 1978; Jaques *et al.*, 1986; Mitchell & Meyer, 1986; Scott-Smith *et al.*, 1989; Mitchell & Bergman, 1991).

may be due to electron beam overlap with adjacent high-Ca phases. Saponite is predominant amongst the secondary groundmass minerals and exhibits a wide compositional range (Table 5). Hydroandradite occurs as inclusions within poikilitic mica and also as fine-grained aggregates in the groundmass. We suspect that hydroandradite and pectolite (Table 5) may have replaced original melilite (but see below) in this rock-type (Skinner *et al.*, 1998). Crystallization of melilite would explain why groundmass phlogopites have lower Al contents than the microphenocrysts (Table 3).

Some of the clasts drilled between 370 and 395 m in the Karpinskiy I diatreme have been classified as olivine lamproites by Mahotkin *et al.* (1995), using the chemical criteria (see below) of Mitchell & Bergman (1991). They have the same abundant olivine macrocrysts and phenocrysts as the associated kimberlites, in a fine-grained

groundmass of red–brown phlogopite, light brown richteritic amphibole and clinopyroxene, lacking both perovskite and hydrogarnet. We emphasize that these rocks are only a very minor and localized part of the AAIP magmatism. The Mela sills are composed of a carbonate-rich variant of kimberlite, comprising serpentinized olivine grains and phlogopite flakes, set in abundant calcite. Locally this becomes carbonatite (Table 1).

Eastern Group kimberlites

Kimberlites in the Eastern Group (Kepino–Pachuga and Verkhotina–Soyana fields) are mica poor, relative to those in the Western Group (Table 1). Phlogopite generally forms 1–7% of the rock and rarely reaches 20%. Perovskite, rutile and Fe–Ti oxides are present as accessory phases in the serpentinized groundmass. Their mineralogy is summarized in Table 1.

The discovery in 1996 of the richly diamondiferous Grib kimberlite pipe (also known as Anomaly 441) has terminated the long-established notion (e.g. Sablukova *et al.*, 1995) that only the AAIP Western Group kimberlites are potentially valuable economically (Verichev *et al.*, 1998; L. Rombouts, personal communication, 1998). The Eastern Group kimberlites are all closely associated with neighbouring diatremes of alkaline picrites (see below).

Alkaline picrites

As the ultramafic diatremes of the AAIP have been discovered and sampled, it has become progressively more apparent that the term kimberlite is inappropriate for all their rock-types, particularly for many in the Verkhotina–Soyana, Kepino–Pachuga and Chidvia groups of diatremes (Fig. 2). Whereas typical AAIP kimberlites (Woolley *et al.*, 1996) are full of rounded olivine macrocrysts, together with other kimberlite indicator minerals (e.g. Kudrjavtseva *et al.*, 1991; Sinitsin *et al.*, 1992; Mahotkin *et al.*, 1995; Sablukova, 1995; Sablukova *et al.*, 1995; Sinitsin & Grib, 1995; Parsadanyan *et al.*, 1996; Griffin *et al.*, 1999) other diatremes contain MgO-rich rock-types that are rich in euhedral or subhedral phenocrysts but poor in rounded macrocrysts. The feature that makes them so difficult to classify is that they contain substantial amounts (up to ~40%) of a former euhedral microphenocryst and groundmass phase that resembles melilite in morphology but has been entirely replaced by aggregates of hydroandradite (± pectolite). As a result, the nomenclature of these enigmatic rocks presents a problem that has to be overcome before their geochemistry and genesis can be discussed without confusion. Their variants have been referred to in several recent publications by such names as olivine melilitite, melilite picrite and melnoite (e.g. Mahotkin *et al.*, 1995; Sinitsin & Grib, 1995; Parsadnayan *et al.*, 1996; Skinner *et al.*, 1998). The problems with such names are that (1) they all imply that fresh melilite occurs in the AAIP whereas, at the time of writing, it has never been analysed by electron microprobe in these rocks (H. Grutter, personal communication, 1999), and (2) mention of AAIP melilitites causes confusion with the contemporaneous melilitites that do indeed contain fresh melilite in the Kandalaksha Gulf (Bell *et al.*, 1996; Beard *et al.*, 1998; Ivanikov *et al.*, 1998), and elsewhere on the Kola Peninsula. We therefore consider that the least controversial approach is to call these AAIP rocks alkaline picrites, following Sinitsin *et al.* (1994).

Figure 4 shows photomicrographs of the alkaline picrites, emphasizing their abundant olivine phenocrysts, relative lack of rounded olivine macrocrysts and the elongate microphenocryst–groundmass pseudomorphs after supposed melilite. We urge extreme caution in the use of the term 'melilitite' in the AAIP, until samples are found in which this mineral is unaltered. Elsewhere worldwide, elongate pseudomorphs and Ca-rich secondary minerals can be seen clearly to replace phlogopite, not melilite, in kimberlitic (*sensu lato*) rocks. For instance, phlogopite-bearing picritic and kimberlitic (*sensu lato*) rock-types in the Alto Paranaíba Igneous Province, SE Brazil, show all stages of phlogopite replacement by calcite (Gibson *et al.*, 1995*a*). The rock-types shown in Fig. 4b and c strongly resemble the phlogopite picrites described by Gibson *et al.* (1995*a*), except that the AAIP elongate microphenocryst and groundmass phase is pseudomorphed by pectolite and hydroandradite, rather than unaltered phlogopite.

The clasts in the Anomaly 651 pipe of the Kepino–Pachuga field (Table 1) typify the alkaline picrites (Fig. 4a, b). They contain 15–20% of euhedral (altered) <3 mm olivine phenocrysts and ~5% chromite microphenocrysts in a formerly microcrystalline to glassy groundmass that is totally altered to fine-grained serpentine, saponite, opaques and hydroandradite. The amounts of pseudomorphs after supposed melilite vary from negligible (Fig. 4a) to abundant (Fig. 4b), from clast to clast. Figure 4c illustrates a variant that is slightly less rich in olivine phenocrysts and contains phlogopite microphenocrysts in a groundmass rich in pseudomorphs after supposed melilite. Clasts of this variant in the Chidvia pipe (Table 1) contain up to several percent of crustal quartz xenocrysts, plus scattered xenocrystal feldspars. Geographically the majority of the alkaline picrites are associated with the Eastern Group of kimberlites (Fig. 2). The micaceous Chidvia picrites occur to the south of the Western Group Zolotitsa kimberlite field. Finally, Table 1 emphasizes an important feature of the AAIP alkaline picrites: most of them are sparsely diamondiferous.

GEOCHEMISTRY

Hydrothermal alteration

All of the investigated samples from the AAIP have been altered to some extent (often substantial) by hydrothermal processes. This common feature of kimberlites and other strongly alkaline provinces is enhanced in the AAIP by the brecciated nature of most rock-types. The extensive array of secondary minerals (Table 1) forms ~20–80% of each rock. Chemical analyses of the alkaline picrites (Table 6) show that they have total volatile contents ($H_2O + CO_2$) of ~6–7%, whereas this value rises to ~7–12% in the kimberlites (excluding their carbonatitic facies in the Mela sills).

We have attempted to evaluate the chemical effects of hydrothermal alteration by comparing analyses of the Pionerskaya diatreme massive kimberlites with those of nearby clasts in the breccias (Table 6). This is not an ideal approach because it cannot disentangle hydrothermal effects from magmatic variations amongst the samples but, nevertheless, it gives an indication of the possible chemical effects of wholesale rather than marginal alteration of the clasts. The only elements strongly affected are Rb, which is dramatically reduced in the altered clasts, and K and Cs, which are reduced substantially in the massive facies. The clasts have higher Si, Na and Ba, and lower Mg, Ca, Cr and Nb, than the massive facies (Table 6). Clearly, variation in such a wide range of elements could have magmatic as well as hydrothermal causes. We consider that the prudent approach, in a province where alteration-free samples are as yet unobtainable, is to treat geochemical variations (except those of K, Rb, Cs and probably Na) as magmatic but to do so with great caution.

Major and trace elements

Two matters need to be emphasized at the beginning of this section: (1) we have only one major-element analysis of a mica-poor Eastern Group kimberlite (Table 6) and therefore also use those published by Parsadanyan *et al.* (1996); (2) we have simplified the discussion below by omitting the kimberlites that are carbonate rich and grade into carbonatites. These are the Mela sills (Table 6) and the Zvezdochka kimberlites of Parsadanyan *et al.* (1996).

The high *mg*-number [Mg/(Mg + Fe)] of the micaceous Western Group kimberlites and lamproites places them together in a distinctive field in variation diagrams (Fig. 6). The Eastern Group kimberlites occupy a lower *mg*-number range (because of higher Fe_2O_3) and also have notably higher TiO_2 than the Western Group kimberlites. There is a varying amount of overlap in the other plots but, in general, kimberlites of the Eastern Group have lower SiO_2 and Lu, and higher Cr, than those in the Western Group. The behaviour of Lu in AAIP rocks is clearly significant, in that this element provides a clear discriminant between kimberlites and all the alkaline picrites, which are relatively Lu rich. Heavy rare earth element (HREE) abundances in rocks containing mantle-derived xenoliths and xenocrysts have to be treated with care, because they can be noticeably affected by small amounts of either fragmented or dissolved xenocrystal mantle garnet. We take the view with the AAIP samples that the consistency of Lu concentrations within each magma group probably means that xenocrystal garnet (Sablukova *et al.*, 1995; Griffin *et al.*, 1999) is not the cause of intergroup Lu variations.

Figure 7 focuses on the AAIP alkaline picrites. A selection of petrographically fresh world-wide melilitites shows that CaO is usually >10% in this rock-type (Fig. 7a), whereas its abundance is much less (as low as 2·85%) in the AAIP samples. At first sight, Fig. 7a suggests that the AAIP alkaline picrites are simply Ca poor as a result of high MgO contents, expressed modally in olivine; all their analyses plot along a trend between typical melilitites and their olivine phenocrysts. Nevertheless, Fig. 7b shows that the situation is more complicated. This plot of ($CaO + Na_2O + K_2O$) vs ($SiO_2 + Al_2O_3$) was proposed by Le Bas (1989) as a discriminant between melilitites, nephelinites and basanites. All of the AAIP alkaline picrites fall far from the melilitite field in this diagram. A vector drawn between a typical Hawaiian melilitite and an appropriate olivine phenocryst composition shows clearly that richness in MgO, expressed as olivine, is not a satisfactory explanation for the anomalous major-element compositions of all the AAIP alkaline picrites. The compositions of the mica-poor picrites might, with difficulty, be fitted by such a model but the Chidvia micaceous picrites clearly have implausibly high ($SiO_2 + Al_2O_3$) contents. We noted above (Table 1) that the Chidvia micaceous picrites contain several percent of xenocrystal quartz, and a vector for quartz addition in Fig. 7b shows that this may explain their compositions. Nevertheless, the amounts of quartz contamination implied by this vector are far higher than the modal quartz in the rocks (<5%). This may be because: (1) several percent of quartz xenocrysts have dissolved in the melts; (2) pervasive hydrothermal alteration has significantly changed the major-element compositions of the AAIP alkaline picrites; (3) the abundant elongate pseudomorphs in these rocks (Fig. 4b, c) may not have originally been melilitite. At present we accept the current view of Skinner *et al.* (1998) that this phase was indeed formerly melilitite. If so, the total pseudomorphic replacement of abundant melilitite in a rock might reasonably be expected to affect relative abundances of SiO_2, Al_2O_3, CaO and alkalis.

The REE are particularly helpful in illuminating the nature and sources of the AAIP magmas. Although even

Table 6: Whole-rock analyses of representative samples from the Late Devonian Arkhangelsk Alkaline Igneous Province

	WESTERN GROUP													
Rock type:	Kimberlite									Olivine lamproite			Kimberlite	
Igneous field:	Zolotitsa	Zolotitsa	Zolotitsa	Zolotitsa	Zolotitsa	Zolotitsa	Zolotitsa	Zolotitsa	Zolotitsa	Zolotitsa	Zolotitsa	Zolotitsa	Mela	Mela
Locality:	Pioner-skaya	Pioner-skaya	Pioner-skaya (altered)	Pioner-skaya (altered)	Lomonosov-skaya	Karpin-skiy II	Karpin-skiy I	Karpin-skiy I	Archangel-skaya	Karpin-skiy I	Karpin-skiy I	Karpin-skiy I	Mela I	Mela I
Sample:	1490/1017	1490/942	1490/1002	1490/987	433/146·3	81/172·7	66/247·3	66/395	505/400	66/395·3	66/370-7	66/370-7a	11/27 2	13/6-1
SiO_2	35·44	39·41	38·83	42·24	36·65	42·02	42·35	45·90	48·83	44·55	38·22	40·20	27·97	27·58
TiO_2	1·08	0·94	0·77	0·83	1·12	0·95	0·85	0·88	0·79	1·30	1·09	1·22	1·02	1·09
Al_2O_3	3·10	2·75	4·95	2·90	2·61	2·22	3·50	3·90	3·91	4·20	4·70	4·80	4·01	4·13
Fe_2O_3	4·50	4·01	1·94	3·38	5·34	5·64	4·10	3·94	5·64	4·55	4·42	4·93	11·46	11·86
FeO	4·16	3·28	4·16	3·78	3·04	3·29	2·95	2·69	1·44	2·42	2·75	2·95	—	—
MnO	0·15	0·14	0·13	0·10	0·14	0·14	0·14	0·17	0·14	0·18	0·15	0·18	0·36	0·41
MgO	31·00	29·67	29·73	27·89	30·27	29·11	29·46	27·53	25·82	28·30	25·33	26·47	23·83	21·76
CaO	6·64	5·60	4·83	5·38	5·75	2·54	2·99	1·42	3·26	1·32	7·35	4·22	12·12	13·34
Na_2O	0·41	0·37	0·86	1·20	0·38	0·58	0·71	0·95	0·50	0·43	0·50	0·42	0·16	0·21
K_2O	2·05	1·13	0·08	0·39	0·71	1·44	1·17	4·22	0·91	5·05	3·90	4·22	0·36	0·46
P_2O_5	0·65	0·46	0·09	0·43	0·54	0·88	0·47	0·21	0·39	0·53	3·70	1·93	0·99	0·87
H_2O^+	0·29	0·51	0·34	0·46	—	0·68	0·60	0·41	0·91	—	—	—	7·35	7·42
H_2O^-	7·00	9·49	11·51	9·08	9·28	9·24	9·00	6·60	5·11	7·04	7·19	7·46	—	—
CO_2	2·37	1·39	0·46	1·21	3·10	0·62	0·75	0·10	1·35	0·10	0·52	0·31	9·77	10·00
Total	98·84	99·15	98·68	99·27	99·35	99·35	99·04	98·92	99·00	99·97	99·82	99·31	99·40	99·13
Ba	1062	442	1710	1250	621	460	1177	960	625	2726	1534	1587	1570	1364
Cr	928	1230	500	690	1536	1047	780	670	790	821	1534	1587	1250	960
Cs	1·4	1·0	0·5	0·5	0·5	1·0	0·8	0·7	0·4	2·0	1·7	1·6	1·3	0·5
Cu	71	65	—	—	220	42	40	—	—	17	—	—	—	—
Ga	7	5	—	—	7	5	6	—	—	11	—	—	—	—
Hf	3·46	1·98	—	2·49	2·21	2·64	3·47	4·14	3·26	4·93	—	4·70	1·73	2·28
Nb	67	53	22	22	66	53	59	51	—	90	4·7	4·7	56	46
Ni	997	1085	620	1250	898	1315	912	940	—	626	848	1115	841	841
Pb	7·3	0·9	—	—	34·4	5·7	34·2	—	—	2·2	—	—	—	—
Rb	100	36	4·8	5·5	38	80	59	137	29	179	162	118	19	15

	WESTERN GROUP													
Rock type:	Kimberlite									Olivine lamproite			Kimberlite	
Igneous field:	Zolotitsa	Zolotitsa	Zolotitsa	Zolotitsa	Zolotitsa	Zolotitsa	Zolotitsa	Zolotitsa	Zolotitsa	Zolotitsa	Zolotitsa	Zolotitsa	Mela	Mela
Locality:	Pioner-skaya	Pioner-skaya	Pioner-skaya (altered)	Pioner-skaya (altered)	Lomonosov-skaya	Karpin-skiy II	Karpin-skiy I	Karpin-skiy I	Archangel-skaya	Karpin-skiy I	Karpin-skiy I	Karpin-skiy I	Mela I	Mela I
Sample:	1490/1017	1490/942	1490/1002	1490/987	433/146·3	81/172·7	66/247·3	66/395	505/400	66/395·3	66/370-7	66/370-7a	11/27 2	13/6-1
Sc	10·4	8·5	—	8·3	11·9	9·2	9·2	10·7	8·4	9·6	—	15·0	18·4	9·1
Sr	687	554	500	575	440	670	638	500	345	1045	2877	1621	880	756
Ta	3·02	2·84	—	2·16	3·49	2·51	2·50	2·46	3·26	3·87	—	3·90	4·29	5·92
Th	4·22	3·82	—	4·61	4·88	3·83	4·83	4·97	4·87	6·63	—	7·20	12·70	13·20
U	0·85	0·86	—	0·79	0·66	0·72	1·04	1·29	1·01	1·36	—	1·40	1·05	0·10
V	79	96	—	—	58	70	63	—	—	822	92	93	86	86
Y	11·1	7·8	19·0	14·0	11·8	9·2	11·9	23·0	—	16·5	22·0	24·0	16·0	16·0
Zn	139	102	—	—	106	131	90	—	—	108	—	—	—	—
Zr	146	80	191	90	92	105	141	170	—	211	115	158	88	79
														—
La	44·4	32·3	—	27·2	30·3	38·1	41·6	50·4	27·1	108·3	—	—	104·0	111·0
Ce	79·9	58·8	—	43·0	58·5	66·6	76·6	86·1	54·7	200·3	—	—	151·0	194·0
Pr	8·91	6·59	—		6·80	7·34	8·74	—	—	23·53	—	—	—	—
Nd	32·9	24·7	—	18·9	24·7	27·0	32·7	37·7	27·6	92·0	—	—	57·5	49·9
Sm	5·11	3·75	—	2·84	4·28	4·22	5·12	5·90	4·19	14·88	—	—	8·60	9·30
Eu	1·45	1·00	—	0·77	1·28	1·14	1·40	1·46	1·00	3·90	—	—	2·00	1·87
Gd	3·85	2·62	—		3·36	3·09	3·77	—	—	10·22	—	—	—	—
Tb	0·49	0·34	—	0·45	0·47	0·40	0·49	0·66	0·48	1·07	—	—	—	—
Dy	2·29	1·55	—		2·37	1·91	2·32	—	—	4·41	—	—	—	—
Ho	0·38	0·27	—	0·52	0·42	0·33	0·41	0·45	0·57	0·68	—	—	—	—
Er	0·91	0·65	—		0·96	0·78	0·98	—	—	1·51	—	—	—	—
Tm	0·12	0·09	—		0·13	0·11	0·15	—	—	0·19	—	—	—	—
Yb	0·72	0·53	—	0·88	0·65	0·64	0·84	1·04	1·02	1·01	—	—	1·44	0·50
Lu	0·10	0·08	—	0·09	0·09	0·09	0·12	0·12	0·12	0·14	—	—	0·10	0·10

Table 6: continued

	WESTERN GROUP			EASTERN GROUP									
Rock type:	Carbonatite			Kimberlite			Mica-poor alkaline picrite				Micaceous alkaline picrite		
Igneous field:	Mela	Mela	Mela	Verkhotina	Pachuga	Pachuga	Pachuga	Pachuga	Pachuga	Pachuga	Chidvia	Chidvia	Chidvia
Locality:	Mela I	Mela III	Mela III	Anomaly 691	Anomaly 693	Anomaly 695	Anomaly 840	Anomaly 651	Anomaly 651	Anomaly 651	Chidvia	Chidvia	Chidvia
Sample:	11/42-2	43/8	43/18	1611/129	3215/160	4008/130	4057/110	711/152	711/226	711/303·5	748/85	748/95	748/120
SiO_2	7·40	8·60	5·01	—	35·47	—	—	45·20	43·10	42·00	50·75	47·60	46·10
TiO_2	0·54	0·72	0·56	3·38	2·75	4·44	3·23	3·40	3·54	3·71	1·13	1·28	0·97
Al_2O_3	2·05	3·80	0·60	—	2·07	—	—	3·90	5·65	4·95	5·75	6·15	5·40
Fe_2O_3	5·06	2·77	1·96	—	10·08	—	—	8·71	8·29	12·31	4·50	6·60	6·35
FeO	0·40	0·48	0·22	—	—	—	—	3·53	3·59	2·58	2·65	2·65	3·75
MnO	0·68	1·02	1·08	0·17	0·29	0·17	0·17	0·12	0·12	0·10	0·09	0·12	0·19
MgO	5·99	7·96	4·59	—	34·08	—	—	22·62	22·77	21·00	21·09	19·57	19·54
CaO	40·84	38·65	45·76	—	1·25	—	—	2·85	3·18	3·35	3·40	4·39	8·12
Na_2O	0·16	0·10	0·20	—	0·10	—	—	0·17	0·16	0·23	2·34	1·48	1·36
K_2O	0·53	0·15	0·19	—	0·39	—	—	0·34	0·22	0·17	1·09	1·65	1·50
P_2O_5	2·42	1·15	4·61	—	0·34	—	—	0·65	0·94	0·79	0·87	0·97	0·82
H_2O^+	3·06	3·86	2·78	—	—	—	—	3·16	3·08	4·70	3·15	4·32	4·23
H_2O^-	0·29	0·29	0·36	—	[12·60]	—	—	3·34	4·22	2·03	1·35	1·72	1·17
CO_2	30·86	31·00	32·50	—	—	—	—	0·81	0·29	0·92	0·75	0·52	0·52
Total	100·28	100·55	100·42	—	99·42	—	—	98·80	99·15	98·84	98·91	99·02	100·02
Ba	2557	430	1125	1051	523	1962	1073	167	975	493	441	869	1185
Cr	455	1048	312	1941	2048	1392	2119	2260	2330	1640	780	930	496
Cs	0·3	0·5	0·7	0·2	1·1	1·2	0·4	—	—	0·1	—	—	2·3
Cu	—	—	—	93	31	21	100	—	—	20	—	—	132
Ga	—	—	—	10	7	14	16	—	—	7	—	—	7
Hf	3·00	—	—	4·51	4·21	10·89	6·98	—	—	6·36	3·50	2·93	2·47
Nb	81	56	141	224	169	347	302	121	137	240	35	41	59
Ni	188	170	38	923	1131	1004	670	1800	1180	864	487	692	446
Pb	—	—	—	6·5	19·9	18·9	11·9	—	—	23·6	—	—	9·0
Rb	19	4·0	4·0	27	36	79	36	18	11	7·0	13	25	71

	WESTERN GROUP			EASTERN GROUP									
Rock type:	Carbonatite			Kimberlite			Mica-poor alkaline picrite				Micaceous alkaline picrite		
Igneous field:	Mela	Mela	Mela	Verkhotina	Pachuga	Pachuga	Pachuga	Pachuga	Pachuga	Pachuga	Chidvia	Chidvia	Chidvia
Locality:	Mela I	Mela III	Mela III	Anomaly 691	Anomaly 693	Anomaly 695	Anomaly 840	Anomaly 651	Anomaly 651	Anomaly 651	Chidvia	Chidvia	Chidvia
Sample:	11/42-2	43/8	43/18	1611/129	3215/160	4008/130	4057/110	711/152	711/226	711/303·5	748/85	748/95	748/120
Sc	9·1	16·7	16·6	18·2	17·8	28·0	27·0	—	—	22·9	17·4	17·1	15·9
Sr	1794	610	1562	389	416	661	704	184	264	448	268	406	547
Ta	5·20	2·70	9·20	16·00	12·19	21·15	18·67	—	—	15·84	2·07	1·91	2·64
Th	22·00	16·70	71·70	13·92	10·17	25·50	21·40	—	—	16·22	5·02	4·78	4·71
U	5·90	4·40	15·40	3·18	2·87	5·85	4·96	—	—	3·15	2·27	2·24	0·78
V	86	74	74	225	206	117	166	—	—	—	—	—	122
Y	23·0	17·0	33·0	19·4	6·1	16·7	25·9	15·0	24·0	28·0	17·0	24·0	17·9
Zn	—	—	—	94	189	828	136	—	—	127	—	—	114
Zr	75	85	134	179	168	465	282	181	214	260	124	120	99
	—	—	—										
La	229·0	154·0	471·0	94·2	57·8	192·2	53·5	—	32·8	40·8	35·3	32·0	41·6
Ce	330·0	222·0	781·0	212·6	109·6	346·0	87·7	—	—	105·9	62·6	62·6	75·6
Pr	—	—	—	28·20	12·95	40·45	16·71	—	—	15·18	—	—	8·40
Nd	—	—	—	110·5	46·3	138·9	63·9	—	36·2	63·8	29·3	28·5	31·2
Sm	14·10	10·50	36·10	16·89	6·38	16·92	9·85	—	6·02	11·60	5·03	5·18	5·51
Eu	3·50	2·80	9·00	4·16	1·60	4·07	2·47	—	—	2·87	1·30	1·50	1·57
Gd	—	—	2·70	11·19	3·44	9·11	6·97	—	—	8·55	—	—	4·45
Tb	—	—	—	1·21	0·42	1·06	0·92	—	—	1·16	0·89	0·82	0·64
Dy	—	—	—	4·67	1·69	4·35	4·80	—	—	5·81	—	—	3·36
Ho	—	—	—	0·66	0·25	0·64	0·88	—	—	1·00	0·66	0·73	0·62
Er	—	—	—	1·29	0·56	1·43	2·36	—	—	2·46	—	—	1·59
Tm	—	—	—	0·15	0·08	0·19	0·37	—	—	0·34	—	—	0·23
Yb	1·90	0·67	0·61	0·78	0·44	1·08	2·14	—	1·80	1·87	1·36	1·51	1·32
Lu	0·33	0·09	0·30	0·11	0·06	0·15	0·32	—	—	0·26	0·17	0·20	0·19

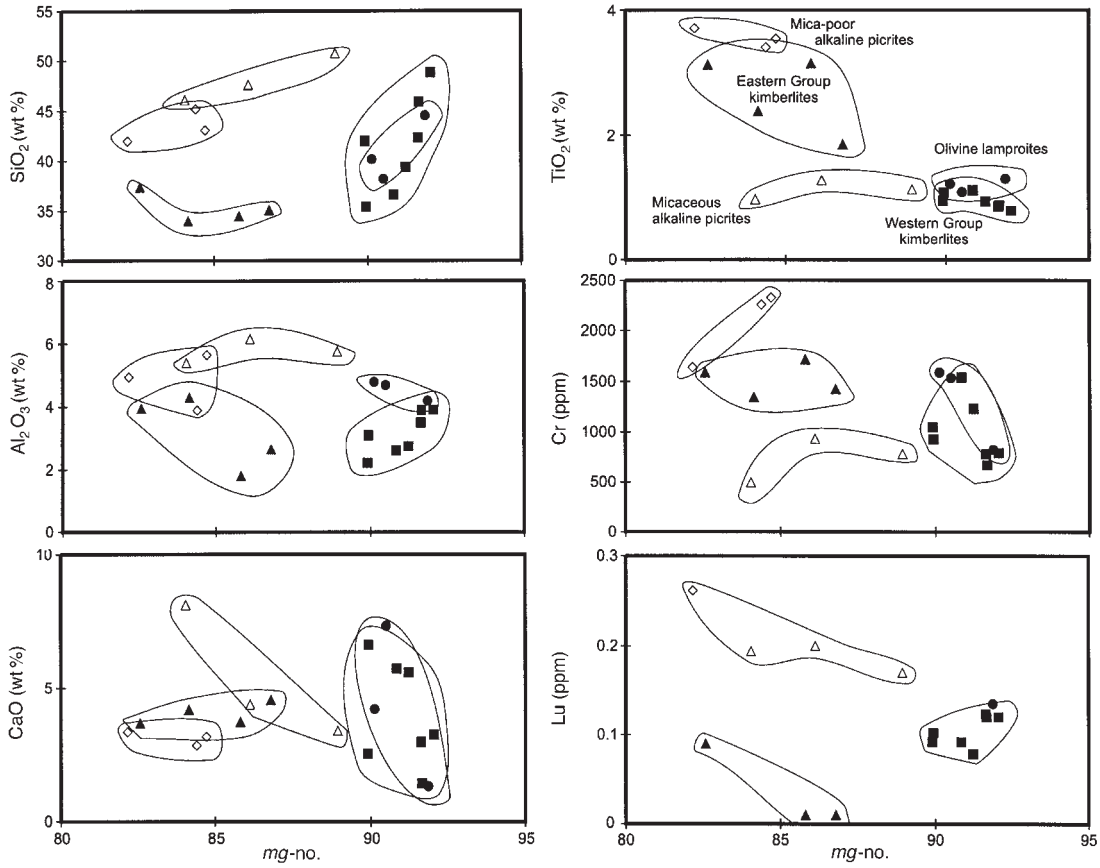

Fig. 6. Variation of *mg*-number with selected major and trace elements in the Late Devonian intrusive igneous rocks (excluding carbonatites) of the AAIP. Data are from Table 6, except for the Eastern Group kimberlites, where analyses from Parsadanyan *et al.* (1996) are also plotted. ■, Western Group kimberlites; ●, olivine lamproites; ▲, Eastern Group kimberlites; ◇, mica-poor alkaline picrites; △, micaceous alkaline picrites.

these elements are sometimes mobile during hydrothermal alteration of mafic–ultramafic rocks (Lahaye *et al.*, 1995), we consider that their relative abundances in these samples may still be magmatic because, in most samples, the alteration has not strongly affected such REE host minerals as perovskite, phlogopite and clinopyroxene. Figure 8 shows REE data for representative samples, grouped according to their localities. The micaceous kimberlites of the Zolotitsa field (Western Group) all have similar REE patterns that are steep and slightly concave upwards. The steepness of the Karpinskiy I lamproite pattern is similar to those of the mica-poor kimberlites from the Verkhotina–Soyana and Kepino–Pachuga fields. The lamproite, however, has a relatively straight pattern, for REE lighter than Ho, whereas the mica-poor (Eastern Group) kimberlite patterns are sigmoidal to varying extents.

Despite their close field association, the mica-poor alkaline picrites have REE patterns that are clearly different from those of the Eastern Group kimberlites. Although sigmoidal, the picrite patterns are less steep and with much higher HREE than the kimberlites (see also Fig. 6). The Chidvia micaceous alkaline picrite has an REE pattern with a similar slope to that for the mica-poor alkaline picrites but concave upwards, rather than sigmoidal. Figure 9a shows a wide range of normalized incompatible elements in representative samples of the main strongly alkaline AAIP rock-types. A basanite (RTH31) from Oahu, Hawaii, is also plotted for comparison. The typical ocean-island basalt (OIB) pattern of this sample is convex upwards, peaking at Nb and Ta. The representative AAIP Eastern Group kimberlite and mica-poor alkaline picrite also have essentially OIB-like patterns, once allowance has been made for hydrothermal stripping of Rb and K. The troughs at Sr in both patterns are a fairly common feature of fresh plagioclase-free mafic–ultramafic strongly alkaline rocks (e.g. Foley *et al.*, 1987). The Western Group kimberlite also has an OIB-like pattern but with a peak at P. The lamproite pattern, overall, does not culminate at Nb and Ta, and shows relative enrichment in Ba, Rb and K, together with a trough at Ti. In Fig. 9b the normalized incompatible

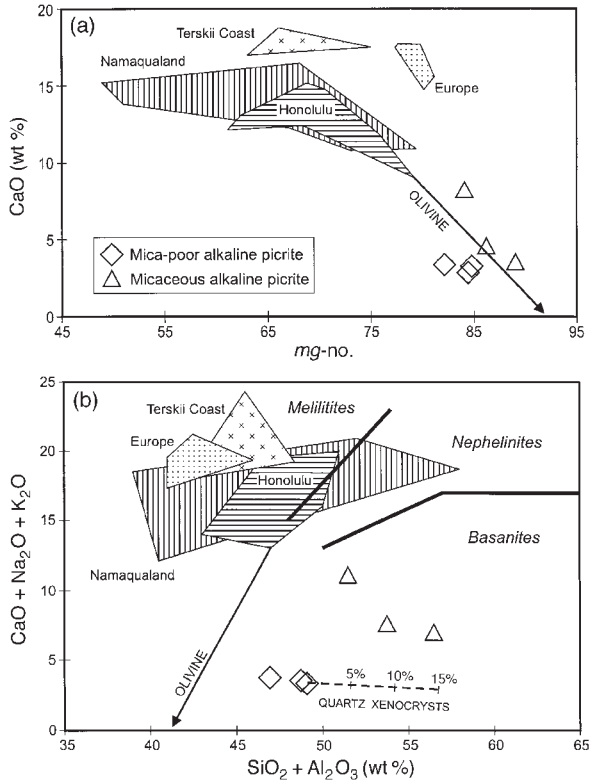

Fig. 7. Comparison of the compositions of alkaline picrites (supposed to have contained melilite) from Arkhangelsk with world-wide melilitite occurrences. (a) *mg*-number vs CaO. (b) $SiO_2 + Al_2O_3$ vs CaO + Na_2O + K_2O diagram for the classification of melilitites, nephelinites and basanites (from Le Bas, 1989). Data sources: Clague & Frey (1982); Hegner *et al.* (1985); Rogers *et al.* (1992), Beard *et al.* (1998); Table 6. Arrows in (a) and (b) show the effect of adding phenocryst olivine to a Honolulu melilitite. Dashed line in (b) shows the effect of adding quartz to an AAIP alkaline picrite (see text).

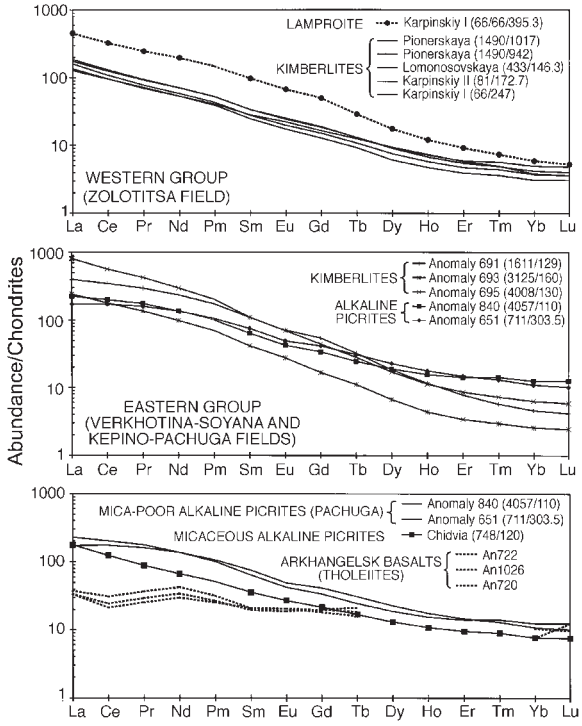

Fig. 8. Chondrite-normalized (Sun & McDonough, 1989) REE patterns for AAIP rock-types (excluding carbonatites). ICP-MS data are from Table 6. Partial patterns (dotted) for Arkhangelsk Late Devonian tholeiitic basalts are from Parsadanyan *et al.* (1996).

trace elements of the two types of AAIP alkaline picrites are compared with those of melilitites from the nearby Terskii Coast, Germany (Hegau) and Brazil (Lages). They are clearly very similar, once allowance has been made for the possible effects of hydrothermal alteration on abundances of Rb and K (also Ba and Sr?) in the AAIP samples. The incompatible element differences between the Chidvia micaceous alkaline picrite and the other mica-poor alkaline picrites (e.g. relatively low Zr, Hf and Ti) give the composition of the Chidvia sample resemblances to those of the nearby Zolotitsa field Western Group kimberlites.

Sr and Nd isotopes

Figure 10 shows a plot of εNd_{380} vs initial $^{87}Sr/^{86}Sr$ for AAIP samples (Table 7), together with the fields of various other oceanic basalts, kimberlites and mafic ultrapotassic rock-types for comparison. The AAIP data form a rather scattered distribution in Fig. 10. Nevertheless, this scatter is not a random one and we think that it contains considerable information about the origin and evolution of the magmas. We have emphasized above that many of the AAIP samples are intensely hydrothermally altered and some have both petrographic and elemental evidence of crustal (sediment) contamination. Both these processes can raise $^{87}Sr/^{86}Sr$ but, for reasons of mass balance, do not normally change εNd significantly in strongly alkaline igneous rocks. In both Table 7 and Fig. 10 it is clear that samples with relatively high $^{87}Sr/^{86}Sr$ occur sporadically; i.e. members of the various AAIP rock-types in Table 7 fall in small and distinctive ranges of εNd, whereas those of $^{87}Sr/^{86}Sr_i$ are larger and values of >0·706 occur in both positive and negative εNd sub-groups.

Table 7 and Fig. 10 show how the AAIP Eastern Group kimberlites and mica-poor alkaline picrites both lie within a small range of positive εNd values. The mica-poor alkaline picrite range (εNd = 0 to +0·9) may possibly be slightly lower than that of the Eastern Group kimberlites (εNd = 0 to +2·5 but with only one sample <1·0). Further data would be needed to confirm this point. All the other AAIP samples that we have studied show negative εNd values but, again, each individual rock-type falls within a small εNd range. Amongst the

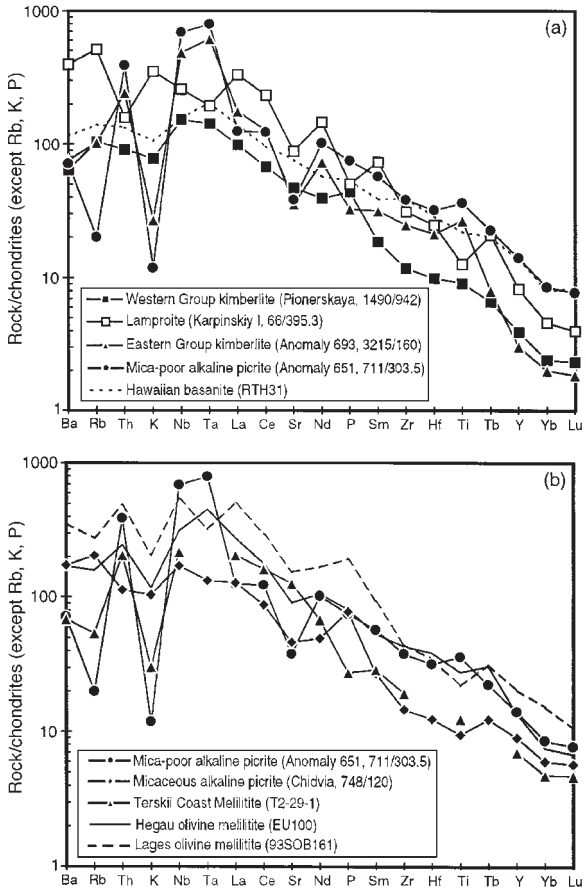

Fig. 9. Normalized multi-element plots for representative examples of the major AAIP rock-types, together with comparable data for a basanite and melilitites from elsewhere (Thompson *et al.*, 1984; Beard *et al.*, 1998; Gibson *et al.*, 1999). Normalization factors are from Thompson *et al.* (1984).

AAIP kimberlites and olivine lamproites, there is a sequence of rising K_2O (despite hydrothermal alteration problems) and falling εNd, as follows: (1) Eastern Group kimberlites, $K_2O = 0{\cdot}21$–$1{\cdot}59$, $\varepsilon Nd = +1{\cdot}1$ to $+2{\cdot}5$; (2) Western Group kimberlites, $K_2O = 0{\cdot}71$–$4{\cdot}22$, $\varepsilon Nd = -2{\cdot}5$ to $-3{\cdot}8$; (3) olivine lamproites, $K_2O = 3{\cdot}90$–$5{\cdot}05$, $\varepsilon Nd = -4{\cdot}6$ to $-4{\cdot}7$. This correlation breaks down when the phlogopite–calcite kimberlites and their closely associated carbonatites are considered. Despite comparatively low K_2O contents, these rock groups have substantially lower εNd values (apart from one Mela carbonatite) than all the kimberlites and olivine lamproites.

The micaceous alkaline picrites plot fairly close to the Western Group kimberlites and olivine lamproites in Fig. 10, at slightly lower εNd values. Thus in terms of Sr–Nd isotope systematics, as with their elemental compositions, these picrites seem to be more similar to the Western rather than the Eastern Group kimberlites. If this grouping is correct, it appears that each kimberlite type has an associated alkaline picrite type that resembles it geochemically, except for relatively less-steep REE patterns and more-abundant HREE.

In Fig. 10 we have also plotted Late Devonian carbonatites from the Kola Peninsula (Kramm *et al.*, 1993) because these extend the AAIP range of εNd to high values, appropriate, for instance, to OIB plume-derived melts resembling those of Hawaii or Iceland. We have drawn a tentative vector in Fig. 10, linking the Kola carbonatites with highest εNd to AAIP kimberlites and alkaline picrites with the lowest $^{87}Sr/^{86}Sr_i$ values in each rock-type. This trend is clearly towards an isotopic component, rich in carbonate and phlogopite with low time-integrated Sm–Nd and Rb–Sr ratios.

DISCUSSION

Tectonic setting of the AAIP diatremes: lithospheric thickness variations and characteristics

The regional tectonic map (Fig. 1) gives firm boundaries to the Archaean Kola craton and the Proterozoic rifts beneath the AAIP. Nevertheless, it must be remembered that all these basement features are entirely hidden beneath a younger sedimentary cover, up to several kilometres thick. Figure 2 shows that the kimberlites and their associated alkaline picrites are confined to a clearly defined region that is surrounded to the south and east by basaltic (*sensu lato*) pipes. Furthermore, the kimberlite and picrite pipes, including those of the Chidvia field, are mostly diamondiferous to varying extents (Table 1). The *P*–*T* constraints of the diamond stability field mean that the lithospheric thickness must average >130 km (see below) beneath the diamondiferous pipes. Thus, Fig. 2 appears to map the SE corner of the buried Kola craton.

The juxtaposition of diamondiferous and basaltic (*sensu lato*) pipes within a few kilometres of each other (Fig. 2; see also Sablukova *et al.*, 1995, Fig. 2) is of considerable theoretical importance in understanding the nature of craton margins adjacent to subsequent rifts. This, in turn, is relevant to successful diamond exploration. In contrast to the ~150 km lithospheric thickness required for diamondiferous magmas, tholeiitic to alkali–olivine basalts (products of relatively dry mantle melting) cannot form deeper than ~125 km, even above the axis of a powerful hot mantle plume (e.g. McKenzie & Bickle, 1988; Farnetani & Richards, 1994). Indeed, if Hawaii is taken as one of the hottest current mantle plumes, it appears that ~75 km is a more realistic value for the maximum lithospheric thickness during tholeiite and alkali–olivine basalt genesis (Watson & McKenzie, 1991). Therefore we

Table 7: Sr- and Nd-isotopic ratios of representative samples of kimberlites and associated rock-types from the Arkhangelsk Alkaline Igneous Province

	Sr	Rb	$^{87}Sr/^{86}Sr_m$	$^{87}Sr/^{86}Sr_i$	Nd	Sm	$^{143}Nd/^{144}Nd_m$	$^{143}Nd/^{144}Nd_i$	εNd_t
Western Group									
Kimberlites									
Pionerskaya (1490/1017)	687	100	0·70609	0·70390	32·9	5·11	0·51225	0·51202	−2·9
Pionerskaya (1490/942)	554	36	0·70667	0·70567	24·7	3·75	0·51227	0·51204	−2·4
Lomonosovskaya (433/146·3)	440	38	0·70670	0·70537	24·7	4·28	0·51228	0·51202	−2·8
Karpinskiy-II (81/172·7)	670	80	0·70613	0·70432	27·0	4·22	0·51223	0·51197	−3·2
Karpinskiy-I (66/247·3)	638	59	0·70503	0·70362	32·7	5·12	0·51221	0·51198	−3·6
Mela-I (11/27-2)	880	19	0·70417	0·70389	57·5	8·60	0·51207	0·51186	−6·0
Anomaly 401 (1500/200a)	709	36	0·70600	0·70523	40·1	6·70	0·51202	0·51177	−7·6
Olivine lamproites									
Karpinskiy-I (66/370·7a)	1621	118	0·70584	0·70436	75·1	11·1	0·51215	0·51193	−4·6
Karpinskiy-I (66/395·3)	1045	179	0·70717	0·70456	92·0	14·8	0·51216	0·51192	−4·7
Carbonatites									
Mela-I (11/42-2)	1794	19	0·70388	0·70369	109·4	14·1	0·51212	0·51192	−4·7
Mela-III (43/8)	610	4·0	0·70476	0·70463	79·3	10·5	0·51205	0·51186	−5·9
Mela-III (43/18)	1562	4·0	0·70381	0·70376	268·8	36·1	0·51206	0·51187	−5·7
Eastern Group									
Kimberlites									
Anomaly 688 (3212/125)	472	35	0·70631	0·70518	30·4	5·50	0·51243	0·51216	0·0
Anomaly 691 (1611/129·7)	389	27	0·70531	0·70423	110·5	16·9	0·51244	0·51222	1·1
Anomaly 693 (3215/160·1)	416	36	0·70498	0·70366	46·3	6·38	0·51248	0·51227	2·2
Anomaly 695 (4008/130)	661	79	0·70580	0·70411	138·9	16·9	0·51242	0·51224	1·5
Anomaly 734 (734·2/153)	465	40	0·70591	0·70460	41·6	5·30	0·51248	0·51229	2·5
Mica-poor alkaline picrites									
Anomaly 651 (711/226)	264	11·0	0·70793	0·70729	36·2	6·02	0·51244	0·51219	0·6
Anomaly 651 (711/303·5)	448	7·0	0·70556	0·70533	63·8	11·8	0·51244	0·51217	0·1
Anomaly 840 (4057/110·4)	704	36	0·70499	0·70426	63·9	9·85	0·51244	0·51221	1·0
Pobeda (1169/70·1)	790	33	0·70561	0·70498	65·0	11·0	0·51247	0·51222	1·1
Micaceous alkaline picrites									
Anomaly 401 (1500/2008)	377	42	0·70716	0·70546	25·0	4·31	0·51213	0·51188	−5·6
Chidvia (748/120)	547	71	0·70696	0·70498	31·2	5·51	0·51214	0·51189	−5·4
Aprelskaya (361/315·5)	439	36	0·70502	0·70378	60·7	9·81	0·51207	0·51183	−6·4

Initial $^{87}Sr/^{86}Sr$ and εNd_t are calculated at 380 Ma.

suspect that lithospheric thickness changes very abruptly between the diamondiferous kimberlite and alkaline picrite to the west and basalts (*sensu lato*) to the east (Fig. 2).

Amongst the AAIP diatremes of predominantly diamondiferous rock-types there is a spatial distribution of chemical variants that has been recognized for a decade in the published literature (e.g. Sablukov, 1990; Mahotkin *et al.*, 1995, 1997; Sablukova *et al.*, 1995). Figure 6 shows that the Western Group kimberlites, olivine lamproites and micaceous alkaline picrites are relatively Ti poor, whereas the Eastern Group kimberlites and mica-poor alkaline picrites are relatively Ti rich. Apart from the Chidvia micaceous alkaline picrites, the two groups also differ substantially in Fe contents (Table 6) and hence *mg*-number; the Eastern Group kimberlites are called Fe–Ti kimberlites in many published accounts. It is apparent in Fig. 2 that these two geochemical sub-types

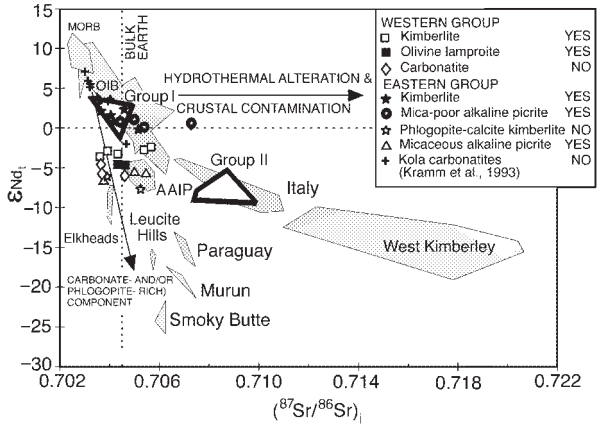

Fig. 10. Comparison of initial $^{87}Sr/^{86}Sr$ and εNd values (Table 7) of the AAIP with other world-wide provinces of mafic ultrapotassic–alkaline rocks. Groups I and II refer to South African kimberlites (Smith, 1983). The fields of present-day mid-ocean-ridge basalts (MORB) and ocean-island basalts (OIB) are shown for reference. Additional data sources: Hawkesworth & Vollmer (1979); Vollmer *et al.* (1984); Rogers *et al.* (1985); Fraser (1987); Ito *et al.* (1987); Davies & Lloyd (1989); Thompson *et al.* (1990); Kramm *et al.* (1993); Mitchell *et al.* (1994); Gibson *et al.* (1995*a*, 1995*b*). (See text for discussion of the arrows.) The words YES and NO in the diagram answer the question: 'Is this rock-type diamondiferous?'

occur within a few kilometres of each other, in two roughly N–S elongated zones, separated by a line at ~41°20′E.The only small-scale exception to this geographical grouping is Anomaly 401 and some adjacent diatremes. These lie to the east of the ~41°20′E line but contain rock-types that classify with the Western Group kimberlites.

Sablukova *et al.* (1995) have focused on these Ti-rich and Ti-poor variants in the Zolotitsa, Soyana and Pachuga pipe fields, making extensive electron- and proton-microprobe analyses of megacryst minerals and fragments in 12 kimberlites. They applied established geothermometry and geobarometry techniques to data for Cr-pyrope garnet and chromite grains. From these results they deduced the following radically different Late Devonian conditions within the lithospheric mantle beneath the Western and Eastern Group kimberlites, despite their proximity (Fig. 2):

(1) beneath the Zolotitsa field (Western Group) kimberlites the Devonian lithosphere consisted of relatively depleted harzburgite, with phlogopite-dominated metasomatism between 125 and 150 km and minor melt-related metasomatism (Harte, 1983; Green & Pearson, 1986; Harte *et al.*, 1993) at depths >160 km. The palaeogeotherm is relatively cool (~37 mW/m^2 using a conductive model), reaching ≤1100°C at ~180 km.

(2) Beneath the Soyana and Pachuga fields (Eastern Group) kimberlites the Devonian lithosphere was also composed of relatively depleted harzburgite but this was extensively affected throughout by melt-related metasomatism. The palaeogeotherm is hotter than that beneath the Western Group kimberlites, reaching ~1300°C at ~180 km.

Kimberlite genesis and evolution

It is clear from our descriptions above that the Eastern and Western kimberlite groups of the AAIP show chemical resemblance to the South African Group I and II kimberlites. The questions that we seek to answer in this section are: (1) Were any of the AAIP kimberlites ever all-liquid magmas and, if so, at what *P*, *T*, etc. did they originate? (2) If not, how far can we disentangle the various contributions to their erupted bulk compositions? These factors and questions are similar to those in recent discussions of South African kimberlites. It is therefore appropriate first to summarize current and recent ideas about the latter:

(1) it has been proposed that at least some South African kimberlites were originally all-liquid magmas, so that the *P*–*T* conditions of their genesis can potentially be defined by experimental petrology, REE inversion or both (e.g. Edgar & Charbonneau, 1993; Tainton & McKenzie, 1994; Dalton & Presnall, 1998). The difference between the Group I and II variants in such magmas could lie in geochemically different types of plumes (spatially or temporally) in the convecting mantle beneath the Kaapvaal craton (Le Roex, 1986).

(2) Many workers have commented on the elemental and isotopic similarities between South African Group I kimberlites and strongly alkaline OIBs, such as the Honolulu Series, Oahu, Hawaii (e.g. Thompson *et al.*, 1984). These similarities are often considered to exist because the Group I kimberlites originated from convecting mantle sources, beneath the Kaapvaal craton. In contrast, the Group II kimberlites do not resemble any oceanic magmas geochemically and may therefore have partially or entirely lithospheric sources.

(3) Studies of osmium and hafnium isotopes in kimberlites favour the view that both Group I and II South African kimberlites have substantial contributions from lithospheric mantle; they all seem to be mixtures from sources both within and beneath the Kaapvaal craton (Pearson *et al.*, 1995; Nowell & Pearson, 1998).

Sablukova *et al.* (1995) emphasized that both mica-poor and micaceous kimberlite in the AAIP are full of finely comminuted crystalline lithospheric material. Therefore option (3) above seems to be the most appropriate way to approach the genesis of these kimberlites. This implies that neither their bulk compositions nor their REE can be used to define specific *P*–*T* conditions for their genesis because they were never entirely liquid melts. Previous studies on AAIP and Terskii Coast kimberlites (Mahotkin *et al.*, 1995, 1997; Parsadanyan *et al.*,

1996; Beard *et al.*, 1998) have treated the rocks as having once been all-liquid melts that could be traced by geochemistry to specific mantle sources. We consider that each kimberlite had no specific 'source' but was assembled from both liquid and solid contributions from various depths, during magma upwelling. Sablukova *et al.* (1995) suggested that the elemental differences between the two AAIP kimberlite types relate to their contrasting lithospheric-source components: phlogopite-dominated metasomatized harzburgites for the micaceous kimberlites; ilmenite-dominated, pervasively melt-invaded harzburgite for the mica-poor kimberlites. This type of model is concordant with the complex morphologies and multistage growth histories of AAIP diamonds (Garanin *et al.*, 1998).

Isotopic data can also help to clarify the situation (especially Nd isotopes, where the effects of hydrothermal alteration and crustal contamination are minimized). The low εNd values of the AAIP Western Group kimberlites place most of them far outside the OIB field in Fig. 10 and the olivine lamproites have slightly lower εNd. These data are concordant with the view that the component that gave the Western Group kimberlites and olivine lamproites their distinctive elemental and isotopic compositions was phlogopite rich and had resided in the lithosphere, isolated from the convecting mantle, for a considerable time. Because the Eastern Group kimberlites have εNd values at and slightly above Bulk Earth, mostly within the OIB field (Fig. 10), it could be argued that these were simply melts from sub-lithospheric convecting mantle. The data of Sablukova *et al.* (1995) show that this cannot be so, and we concur with these workers that the simplest explanation of the isotopic data is that upwelling melts from sub-lithospheric sources incorporated crystalline debris from previous magma batches, which had reacted with and frozen within the lithosphere only a comparatively short time previously. This genetic scheme is very similar to the one proposed for some OIBs by McKenzie & O'Nions (1995). Sablukova *et al.* (1995) supported this view because their reconstructed palaeogeotherm for the Eastern Group kimberlites is steepened in the lower lithosphere. This is consistent with advective heat transfer into the lithosphere, from the underlying convecting mantle, shortly before kimberlite genesis. Very similar processes appear to have taken place during the Tertiary in parts of the Tanzanian (Nyanza) craton affected by the mantle plume beneath the East African rift (Chesley *et al.*, 1998; Lee & Rudnick, 1998). Nevertheless, the high εNd of Kola carbonatites (Fig. 10) and most other alkaline igneous rocks on the Kola Peninsula leaves open the less-obvious possibility that the sub-lithospheric contribution to the Arkhangelsk Eastern Group kimberlites also had much higher εNd and that the present values, near Bulk Earth, disguise a substantial lower-εNd lithospheric input.

Is there any direct evidence within the AAIP kimberlites for a sub-lithospheric contribution to the magmas? Sobolev *et al.* (1997) have reported electron microprobe analyses of olivine, chromite, pyroxene and garnet inclusions within AAIP diamonds. Amongst these are a pyrope inclusion containing significant pyroxene solid solution (the first outside South Africa and Brazil) and relatively high K_2O (0·65–0·80%) in jadeite-rich pyroxenes. Both these mineralogical features suggest that their host diamonds originated several hundred kilometres deep, well below the base of the sub-AAIP lithosphere (Haggerty, 1994; Sablukova *et al.*, 1995; Harlow, 1997).

Mahotkin *et al.* (1995, 1997) and Parsadanyan *et al.* (1996) have proposed that a mantle plume may have been the heat source for this widespread Late Devonian melting event. This hypothesis is supported by a recent study of noble gases (He, Xe and Ne) in Devonian carbonatites from the Kola Peninsula, which has shown that they are similar to those of OIBs and that the carbonatites contain primordial rare gases from the lower mantle (Marty *et al.*, 1998). We propose that the Arkhangelsk magmatism is linked to the impact of this same 'Kola' mantle plume.

The alkaline picrites; are they 'protokimberlites'?

Despite the published suggestion that they contain pseudomorphed melilite (discussed above), it needs to be stressed that both the AAIP alkaline picrites are entirely unlike melilitites from well-known suites elsewhere (e.g. Fig. 7). The latter occur in both oceanic and continental settings where the lithospheric thickness is <100 km and they are widely supposed to originate within the lithosphere (Rogers *et al.*, 1992; Hoernle & Schmincke, 1993; Beard *et al.*, 1998; Gibson *et al.*, 1999). Their diamond content places the sources of the AAIP alkaline picrites much deeper. Bearing in mind their εNd values (Fig. 10), there is no obvious reason why they could not have originated in the convecting mantle beneath the Kola craton (i.e. >180 km; Sablukova *et al.*, 1995).

The spatial relationship between the AAIP mica-poor Eastern Group kimberlites and alkaline picrites (Fig. 2) seems too close to be no more than a coincidence, despite such important chemical differences as REE pattern slopes and curvature (Fig. 8). Published accounts of South African kimberlites may clarify the significance of the AAIP alkaline picrites. Almost all South African Group I kimberlites contain large monomineralic megacrysts from a suite of minerals that includes subcalcic clinopyroxene, orthopyroxene, pyrope garnet, ilmenite and zircon. Detailed geochemical studies by Jones (1987) followed up earlier reports (e.g. Harte, 1983) that these

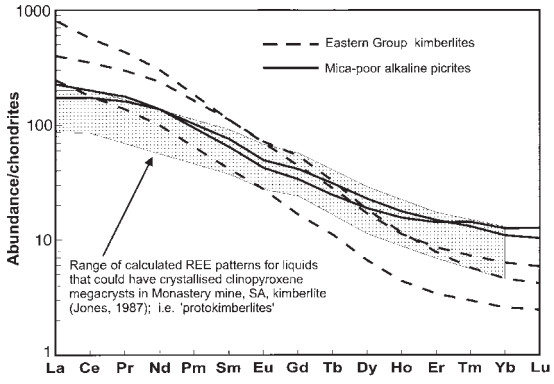

Fig. 11. Chondrite-normalized REE patterns for AAIP Eastern Group kimberlites and alkaline picrites (Table 6), and the range of patterns calculated (Jones, 1987) for South African hypothetical 'protokimberlite'. (See text for details.)

minerals appeared to have crystallized as phenocrysts at depth from a magma, but that this liquid was both elementally and isotopically different from the kimberlites that hosted them. Jones (1987) concentrated on REE in the sub-calcic clinopyroxenes because they are much more REE rich than the other megacryst minerals, but he also showed that the garnets gave concordant results (see also Nowell & Pearson, 1998). When the REE patterns of the magmas that would have been in equilibrium with the sub-calcic clinopyroxene (and garnet) megacrysts were calculated, they were those of oceanic alkali–olivine basalts and basanites; very different from the host kimberlites. Jones (1987) proposed that precursor melts to the Group I kimberlites (called 'protokimberlites' by some researchers) originated within convecting mantle beneath the South African lithosphere. As they rose towards the surface, they evolved towards Group I kimberlite compositions by precipitation of the megacryst phases and incorporation, with partial dissolution, of material from the overlying lithospheric mantle. Figure 11 compares the chondrite-normalized REE patterns of AAIP Eastern Group kimberlites and mica-poor alkaline picrites with the range of 'protokimberlite' REE patterns, calculated by Jones (1987). The similarity between the AAIP alkaline picrite and the hypothetical 'protokimberlite' REE patterns is remarkable. There is a small difference in pattern curvature but it must be emphasized that Jones' calculations used crystal–liquid partition coefficients from a decade ago and that very small changes in the preferred middle REE values will change calculated pattern curvatures considerably.

We suggest that the diamondiferous megacryst-free AAIP mica-poor alkaline picrites are a small missing part of the kimberlite jigsaw puzzle, namely, approximations to the hypothetical 'protokimberlites' that are deduced from megacryst studies to be widespread precursor melts, at sub-lithospheric depths, to South African Group I kimberlites. This suggestion implies that the genetic model of Jones (1987), Pearson *et al.* (1995), Nowell & Pearson (1998), and many others for South African kimberlites may apply equally well to the AAIP. In each case, parts of the petrogenetic jigsaw puzzle are currently missing: in South Africa there are Group I kimberlites and their megacrysts but no recognized 'protokimberlites'; in the AAIP there are Group I kimberlites and 'protokimberlites' (mica-poor alkaline picrites) but no appropriate megacrysts yet described. This problem may soon be resolved because Sablukova *et al.* (1995) noted that the AAIP Eastern Group kimberlites contain abundant Mg–Cr-rich ilmenites that 'show good magmatic fractionation trends', as is often the case in such suites elsewhere (Griffin *et al.*, 1997).

Although our new data are a step towards an improved understanding of AAIP magmatism, we consider that we would be over-interpreting them if we attempted to develop a detailed model of how combined fractional crystallization and lithospheric contamination took place during the evolution of AAIP 'protokimberlite' to mica-poor (Eastern Group) kimberlite. The normalized incompatible-element data plotted in Fig. 9a give one clue about these processes. The normalized patterns of both AAIP mica-poor kimberlite and alkaline picrite show positive spikes at both Ti and (especially) Nb and Ta, when compared with the pattern for a Hawaiian basanite (RTH31; Fig. 9) or OIBs in general. This feature may be expressed differently by comparing Nb/La in worldwide OIBs (average 1·15; Fitton *et al.*, 1991) with values of this ratio in AAIP Eastern Group kimberlites and alkaline picrites (1·8–5·9; Table 6). It seems reasonable to attribute this chemical difference between OIB-like rock-types in the AAIP and true OIBs to ilmenite, rich in Nb and Ta (Griffin *et al.*, 1997), in the AAIP samples; both as solid macrocryst debris and dissolved(?) in the Eastern Group kimberlite, and dissolved in the alkaline picrite. Greenwood *et al.* (2000) identified the same phenomenon in the Paranatinga kimberlites of Brazil. Future detailed geochemical studies of AAIP samples less affected by hydrothermal alteration or crustal contamination, or by both, will be needed to add detail to our tentative genetic model. Such studies will also need to consider whether such a model can be extended to show a genetic relationship between the AAIP Western Group kimberlites and their associated micaceous alkaline picrites.

SUMMARY

(1) The diatremes and sills of the Late Devonian (380–360 Ma) Arkhangelsk Alkaline Igneous Province (AAIP) are part of a larger area of contemporaneous varied magmatism.

(2) AAIP rock-types include kimberlites, olivine lamproites, alkaline picrites (±melilite?) and carbonatites. The carbonatites form components of sills and the other rock-types are fragments in diatremes.

(3) Pervasive hydrothermal alteration makes the role of 'melilite' somewhat uncertain in these rocks because it is entirely pseudomorphed. Nevertheless, there is a clear textural separation between the alkaline picrites and the kimberlites; the latter are full of comminuted megacrysts and lithospheric mantle debris.

(4) Two kimberlite variants occur: predominantly micaceous (Western Group) and predominantly mica poor (Eastern Group). These are <25 km apart. They resemble South African Group I and II kimberlites petrographically and chemically but are far from identical to them.

(5) AAIP Western Group kimberlites and olivine lamproites are diamondiferous (some richly). The Eastern Group kimberlites are generally poorly diamondiferous to barren. The alkaline picrites are sparsely diamondiferous and the carbonatites are barren.

(6) The various rock groups are clearly differentiated by the slopes and shapes of their chondrite-normalized REE patterns. The alkaline picrite patterns are much less steep (with notably higher HREE) than those of either kimberlite type.

(7) Published data (Sablukova *et al.*, 1995) show that both kimberlite types are full of megacryst fragments and lithospheric mantle debris, and that this xenocrystal material is specific to each suite: it is dominated by phlogopite in the Western Group kimberlites, and rich in ilmenite in the Eastern Group kimberlites. Nevertheless, minerals enclosed within AAIP diamonds include pyrope with significant pyroxene solid solution and relatively K-rich jadeiitic pyroxenes (Sobolev *et al.*, 1997), both indicating magma genesis at depths of several hundred kilometres. These data support an AAIP kimberlite genesis model of precursor melts forming in convecting mantle, well beneath the lithosphere; rising through lithospheric mantle with locally variable metasomatic prehistories; and reacting with, dissolving and physically incorporating lithospheric mantle phases, to produce hybrid kimberlite magmas.

(8) The mica-poor alkaline picrite REE patterns are very similar to those of the 'protokimberlite' magmas, calculated to be in equilibrium with sub-calcic clinopyroxene and other megacryst phases in South African Group I kimberlites (Jones, 1987; Nowell & Pearson, 1998). We suspect that this sparsely diamondiferous picrite is a minimally lithosphere-contaminated sample of AAIP deep-source 'protokimberlite' magmas. Nevertheless, even the picrites show evidence of post-genesis complexity. They are relatively enriched in Fe, Ti, Nb and Ta (e.g. Nb/La up to 5·9). If the picrite magma originated from the same convecting mantle source as OIB, it appears subsequently to have dissolved ilmenite.

(9) The widespread broadly synchronous magmatism and abundance of Mg-rich rock-types on the Kola Peninsula and in the AAIP all suggest the impact of a starting mantle plume beneath NW Russia in the Late Devonian. Around Arkhangelsk the pre-existing lithospheric thickness was crucial in controlling how close to the surface the head of the Kola starting plume could rise, and hence the types of magmas that were generated. The end-member products were diamondiferous kimberlites and alkaline picrites on the SE margin of the Kola craton, and tholeiitic basalts where cratonic (>150 km) lithosphere had been thinned by subsequent rifting.

ACKNOWLEDGEMENTS

This work was funded by the International Scientific Foundation (Moscow, Grant N5D000) and financial support from the Universities of Cambridge and Durham. We warmly thank Luc Rombouts and Steve Haggerty for information and discussions on the Arkhangelsk kimberlites. We are grateful to Y. Brown, J. C. Greenwood, R. G. Hardy, J. Keller, C. J. Ottley and D. G. Pearson for their help with analytical equipment and techniques. We would also like to thank H. Aliberti and C. Moseley for their assistance with preparation of this manuscript. Keith Bell, Hilary Downes and Lizzy Ann Dunworth are thanked for their thorough and constructive reviews of an earlier draft of this manuscript.

REFERENCES

Beard, A. D., Downes, H., Vetrin, V., Kempton, P. D. & Maluski, H. (1996). Petrogenesis of Devonian lamprophyre and carbonatite minor intrusions, Kandalaksha Gulf (Kola Peninsula, Russia). *Lithos* **39**, 93–119.

Beard, A. D., Downes, H., Hegner, E., Sablukov, S. M., Vetrin, V. R. & Balogh, K. (1998). Mineralogy and geochemistry of Devonian ultramafic minor intrusions of the Kola Peninsula, Russia: implications for the petrogenesis of kimberlites and melilitites. *Contributions to Mineralogy and Petrology* **130**, 288–303.

Bell, K., Dunworth, E. A., Bulakh, A. G. & Ivanikov, V. V. (1996). Alkaline rocks of the Turiy Peninsula, Russia, including type-locality turjaite and turjite: a review. *Canadian Mineralogist* **34**, 265–280.

Berkovsky, A. N. & Platunova, A. P. (1989) Giant mafic dyke swarms of the East European Craton. *New Mexico Bureau of Mines and Mineral Resources, Bulletin* **131**, 21.

Blundell, D., Freeman, R. & Mueller, S. (1992). *A Continent Revealed: The European Geotraverse*. Cambridge: Cambridge University Press.

Bogdanova, S. V., Pashkevich, I. K., Gorbatschev, R. & Orlyuk, M. I. (1996) Riphean rifting and major Palaeoproterozoic crustal boundaries in the basement of the East European craton: geology and geophysics. *Tectonophysics* **268**, 1–21.

Chesley, J. T., Rudnick, R. L. & Lee, C.-T. (1998). Longevity of cratonic mantle beneath an active rift: Re–Os evidence from xenoliths from the Tanzanian East African rift. *Extended Abstracts: 7th International Kimberlite Conference*. Cape Town: University of Cape Town, pp. 149–151.

Clague, D. A. & Frey, F. A. (1982). Petrology and trace element geochemistry of the Honolulu volcanics, Oahu: implications for the oceanic mantle below Hawaii. *Journal of Petrology* **23**, 447–504.

Dalton, J. A. & Presnall, D. C. (1998). The continuum of primary carbonatitic–kimberlitic melt compositions in equilibrium with lherzolite: data from the system CaO–MgO–Al_2O_3–SiO_2–CO_2 at 6 GPa. *Journal of Petrology* **39**, 1953–1964.

Davies, G. R. & Lloyd, F. E. (1989). Pb–Sr–Nd isotope and trace element data bearing on the origin of the potassic subcontinental lithosphere beneath south-west Uganda. In: Ross, J. (ed.) *Proceedings of the 4th International Kimberlite Conference, Perth. Geological Society of Australia Special Publication* **14**, 785–794.

Dawson, J. B. & Hawthorne, J. B. (1973). Magmatic sedimentation and carbonatitic differentiation in kimberlite sills at Benfontein, South Africa. *Journal of the Geological Society, London* **129**, 61–85.

Dawson, J. B. & Smith, J. V. (1977). The MARID (mica–amphibole–rutile–ilmenite–diopside) suite of xenoliths in kimberlite. *Geochimica et Cosmochimica Acta* **41**, 309–323.

Dudkin, O. B. & Mitrofanov, F. P. (1993). Features of the Kola Alkaline Province. *Geochemistry International* **31**, 1–11.

Edgar, A. D. & Charbonneau, H. E. (1993). Melting experiments on a SiO_2-poor, CaO-rich aphanitic kimberlite from 5–10 GPa and their bearing on sources of kimberlite magmas. *American Mineralogist* **78**, 132–142.

Erinchek, Yu. M., Milshtein, E. D., Saltykov, O. G. & Verzhak, V. V. (1998). Local depressions in country rock of kimberlites as a new exploration criterion: the example of the Zolotitsa field, Arkhangelsk, Russia. *Extended Abstracts: 7th International Kimberlite Conference*. Cape Town: University of Cape Town, pp. 208–210.

Farnetani, C. G. & Richards, M. A. (1994). Numerical investigations of mantle plume initiation model for flood basalt events. *Journal of Geophysical Research* **99**, 13813–13833.

Fitton, J. G., James, D. & Leeman, W. P. (1991). Basic magmatism associated with Late Cenozoic extension in the western United States: compositional variations in space and time. *Journal of Geophysical Research* **96**, 13693–13711.

Foley, S. F., Venturelli, G., Green, D. H. & Toscani, L. (1987). The ultrapotassic rocks: characteristics, classification and constraints for petrogenetic models. *Earth-Science Reviews* **24**, 81–134.

Fraser, K. J. (1987). Petrogenesis of kimberlites from South Africa and lamproites from Western Australia and North America. Ph.D. Thesis, Open University, Milton Keynes, UK.

Garanin, V. K., Kudriavtseva, G. P. & Possukhova, T. V. (1998). Diamonds of Arkhangelsk kimberlite province (review). *Extended Abstracts: 7th International Kimberlite Conference*. Cape Town: University of Cape Town, pp. 233–235.

Gibson, S. A., Thompson, R. N., Leat, P. T., Morrison, M. A., Hendry, G. L., Dickin, A. P. & Mitchell, J. G. (1993). Ultrapotassic magmas along the flanks of the Oligo-Miocene Rio Grande rift, USA: monitors of the zone of lithospheric mantle extension and thinning beneath a continental rift. *Journal of Petrology* **34**, 187–228.

Gibson, S. A., Thompson, R. N., Leonardos, O. H., Dickin, A. P. & Mitchell, J. G. (1995*a*). The Late Cretaceous impact of the Trindade mantle plume: evidence from large-volume, mafic, potassic magmatism in SE Brazil. *Journal of Petrology* **36**, 189–229.

Gibson, S. A., Thompson, R. N., Leonardos, O. H. & Dickin, A. P. (1995*b*). High-Ti and Low-Ti mafic potassic magmas: key to plume–lithosphere interactions and continental flood-basalt genesis. *Earth and Planetary Science Letters* **136**, 149–165.

Gibson, S. A., Thompson, R. N., Leonardos, O. H. & Dickin, A. P. (1999). The limited extent of plume–lithosphere interactions during continental flood basalt genesis: geochemical evidence from Cretaceous magmatism in southern Brazil. *Contributions to Mineralogy and Petrology* **137**, 147–169.

Green, T. H. & Pearson, N. J. (1986). Ti-rich accessory phase saturation in hydrous mafic–felsic composition at high *P,T*. *Chemical Geology* **54**, 185–201.

Greenwood, J. C., Gibson, S. A., Thompson, R. N., Weska, R. K. & Dickin, A. P. (2000). Cretaceous kimberlites from the Paranatinga–Batovi region, central Brazil: geochemical evidence for subcratonic lithospheric mantle heterogeneity. *Proceedings of 7th International Kimberlite Conference*. Cape Town: University of Cape Town (in press).

Grib, V. P., Scripnichenko, V. A. & Shchukin, V. S. (1987). Alkaline-ultramafic magmatism of the northern margin of the Russian platform. In: *Geology and Ore Deposits in the Northern Russian Platform*. Moscow: Geolfond Proceedings, pp. 66–74.

Griffin, W. L., Moore, R. O., Ryan, C. G., Gurney, J. J. & Win, T. T. (1997). Geochemistry of magnesian ilmenite megacrysts from southern African kimberlites. *Russian Geology and Geophysics* **38**, 421–443.

Griffin, W. L., Fisher, N. I., Friedman, J., Ryan, C. G. & O'Reilly, S. Y. (1999). Cr-pyrope garnets in the lithospheric mantle. 1. Compositional systematics and relations to tectonic setting. *Journal of Petrology* **40**, 679–704.

Haggerty, S. E. (1994). Superkimberlites: a geodynamic diamond window to the Earth's core. *Earth and Planetary Science Letters* **122**, 57–69.

Harlow, G. E. (1997). K in clinopyroxene at high pressure and temperature: an experimental study. *American Mineralogist* **82**, 259–269.

Harte, B. (1983). Mantle peridotites and processes—the kimberlite sample. In: Hawkesworth, C. J. & Norry, M. J. (eds) *Continental Basalts and Mantle Xenoliths*. Nantwich, UK: Shiva, pp. 46–91.

Harte, B., Hunter, R. H. & Kinney, P. D. (1993). Melt geometry, movement and crystallisation, in relation to mantle dykes, veins and metasomatism. *Philosophical Transactions of the Royal Society of London, Series A* **342**, 1–21.

Hawkesworth, C. J. & Vollmer, R. (1979). Crustal contamination versus mantle enrichment, $^{143}Nd/^{144}Nd$ and $^{87}Sr/^{86}Sr$ evidence from Italian volcanics. *Contributions to Mineralogy and Petrology* **69**, 151–165.

Hegner, E., Walter, H. J. & Satir, M. (1995). Pb–Sr–Nd isotopic compositions and trace element geochemistry of megacrysts and melilitites from the Tertiary Urach volcanic field: source composition of small volume melts under SW Germany. *Contributions to Mineralogy and Petrology* **122**, 322–335.

Hervig, R. L., Smith, J. V., Steele, I. M., Gurney, J. J., Meyer, H. O. A. & Harris, J. W. (1980) Diamonds: minor elements in silicate inclusions: pressure–temperature implications. *Journal of Geophysical Research* **85**, 6919–6929.

Hoernle, K. A. J. & Schminke, H. U. (1993). The petrology of tholeiites through melilite nephelinites on Gran Canaria, Canary Islands: crystal fractionation, accumulation and depths of melting. *Journal of Petrology* **34**, 573–597.

Ishmail-Zadeh, A. T., Kostyuchenko, S. L. & Naimark, B. M. (1997). The Timan–Pechora basin (northeastern European Russia): tectonic subsidence analysis and a model of formation mechanism. *Tectonophysics* **283**, 205–218.

Ito, E., White, W. M. & Gopel, C. (1987). The O, Sr, Nd and Pb isotope geochemistry of MORB. *Chemical Geology* **62**, 157–176.

Ivanikov, V. V., Rukhlov, A. S. & Bell, K. (1998). Magmatic evolution of the melilitite–carbonatite–nephelinite dyke series of the Turiy Peninsula (Kandalashka Bay, White Sea, Russia). *Journal of Petrology* **39**, 2043–2059.

Jaques, A. L., Lewis, J. D. & Smith, C. B. (1986). The kimberlites and lamproites of western Australia. *Geological Survey of Western Australia Bulletin* **132**, 1–268.

Jones, R. A. (1987). Strontium and neodymium isotope and rare earth element evidence for the genesis of megacrysts in kimberlites of southern Africa. In: Nixon, P. H. (ed.) *Mantle Xenoliths*. New York: John Wiley, pp. 711–724.

Khain, V. E. & Bozhko, N. A. (1988). *The Historical Geotectonics of the Precambrian*. Moscow: Nedra (in Russian).

Kogarko, L. N., Kononova, V. A., Orlova, M. P. & Woolley, A. P. (1995). *Alkaline Rocks and Carbonatites of the World: Part 2: Former USSR*. London: Chapman & Hall.

Konstantinovskiy, A. A. (1977). Onego–Kandalakshskiy Rifean graben of the East-European Platform. *Geotectonica* **3**, 38–45 (in Russian).

Kramm, U., Kogarko, L. N., Kononova, V. A. & Vartianen, H. (1993). The Kola alkaline province of the CIS and Finland: precise Rb–Sr ages define 380–360 Ma age range for all magmatism. *Lithos* **30**, 33–44.

Kudrjavtseva, G. P., Bushueva, E. B., Vasiljeva, E. R., Verichev, E. M., Garanin, V. K. (1991). Geological structure and mineralogy of the kimberlites of the Arkhangelsk kimberlites province. *Extended Abstracts, 5th International Kimberlite Conference, Araxa*. Rio de Janeiro: Companhia de Pesquisa de Recursos Minerais, pp. 530–532.

Lahaye, Y., Arndt, N. T., Byerly, G., Chauvel, C., Foucade, S. & Gruau, G. (1995). The influence of alteration on the trace-element and Nd isotopic compositions of komatiites. *Chemical Geology* **126**, 43–64.

Le Bas, M. J. (1989). Nephelinitic and basanitic rocks. *Journal of Petrology* **30**, 1299–1312.

Lee, C.-T. & Rudnick, R. L. (1998). The origin and demise of cratonic lithosphere: a geochemical perspective from the Tanzanian craton. *Extended Abstracts: 7th International Kimberlite Conference*. Cape Town: University of Cape Town, pp. 492–494.

Le Roex, A. P. (1986). Geochemical correlation between southern African kimberlites and South Atlantic hotspots. *Nature* **324**, 243–245.

Mahotkin, I. L. (1998). Petrology of Group 2 kimberlite–olivine lamproite (K2L) series from the Kostomuksha area, Karelia, N.W. Russia. *Extended Abstracts: 7th International Kimberlite Conference*. Cape Town: University of Cape Town, pp. 529–531.

Mahotkin, I. L., Sablukov, S. M., Zhuravlev, D. Z. & Zherdev, P. U. (1995). Geochemistry and Sr–Nd isotopic composition of kimberlites, melilitites and basalts from the Arkhangelsk region, Russia. *Extended Abstracts: 6th International Kimberlite Conference*. Novosibirsk: United Institute of Geology, Geophysics and Mineralogy, Siberian Branch of the Russian Academy of Sciences Novosibirsk, pp. 342–344.

Mahotkin, I. L., Zhuravlev, D. Z., Sablukov, S. M., Zherdev, P. U., Thompson, R. N. & Gibson, S. A. (1997). Plume–lithosphere interactions as a geodynamic model of origin of the Archangelsk diamondiferous province. *Transactions of the Russian Academy of Science* **353**, 1–5.

Marty, B., Tolstikhin, I., Kamensky, I. L., Nivin, V., Balaganskaya, E. & Zimmermann, J.-L. (1998). Plume-derived rare gases in 380 Ma carbonatites from the Kola region (Russia) and the argon isotopic composition in the deep mantle. *Earth and Planetary Science Letters* **164**, 179–192.

McKenzie, D. P. (1989). Some remarks on the movement of small melt fractions in the mantle. *Earth and Planetary Science Letters* **95**, 53–72.

McKenzie, D. P. & Bickle, M. J. (1988). The volume and composition of melt generated by extension of the lithosphere. *Journal of Petrology* **29**, 625–679.

McKenzie, D. & O'Nions, R. K. (1995). The source regions of ocean island basalts. *Journal of Petrology* **36**, 133–159.

Mitchell, R. H. (1986). *Kimberlites: Mineralogy, Geochemistry, and Petrology*. New York: Plenum.

Mitchell, R. H. & Bergman, S. C. (1991). *Petrology of Lamproites*. New York: Plenum.

Mitchell, R. H. & Meyer, H. O. A. (1986). Mineralogy of micaceous kimberlites from the New Elands and Star Mines. *Extended Abstracts, 4th International Kimberlite Conference, Perth, Geological Society of Australia*. Oxford: Blackwell Scientific, pp. 75–77.

Mitchell, R. H., Smith, C. B. & Vladykin, N. V. (1994). Isotopic composition of strontium and neodymium in potassic rocks of the Little Murun complex, Aldan Shield, Siberia. *Lithos* **32**, 243–248.

Nikishin, A. M., Ziegler, P. A., Stephenson, R. A., Cloetingh, S. A. P. L., Furne, A. V., Fokin, P. A., Ershov, A. V., Bolotov, S. N., Korotaev, M. V., Alekseev, A. S., Gorbachev, V. I., Shipilov, E. V., Lankreijer, J., Bembinova, E. Yu. & Shalimov, I. V. (1996). Late Precambrian to Triassic history of the East European Craton: dynamics of sedimentary basin formation. *Tectonophysics* **268**, 23–63.

Nowell, G. M. & Pearson, D. G. (1998). Hf isotope constraints on the genesis of kimberlitic megacrysts: evidence for a deep mantle component in kimberlites. *Extended Abstracts: 7th International Kimberlite Conference*. Cape Town: University of Cape Town, pp. 634–636.

Parsadanyan, K. S., Kononova, V. A. & Bogatikov, O. A. (1996). Sources of heterogeneous magmatism of the Arkhangelsk diamondiferous province. *Petrology* **4**, 460–479.

Pearson, D. G. (2000). The age of continental roots. *Lithos* (in press).

Pearson, D. G., Carlson, R. W., Shirey, S. B., Boyd, F. R. & Nixon, P. H. (1995). The stabilisation of Archaean lithospheric mantle: a Re–Os isotope study of peridotite xenoliths from the Kaapvaal craton. *Earth and Planetary Science Letters* **134**, 341–357.

Proskuriykov, V. V., Uvadiev, L. I. & Voninova, O. A. (1992). Lamproites of the Karelo–Kola region. *Doklady Akademii Nauk SSSR* **314**, 940–943 (in Russian).

Rogers, N. W., Hawkesworth, C. J., Parker, R. J. & Marsh, J. S. (1985). The geochemistry of potassic lavas from Vulsini, central Italy, and implications for mantle enrichment processes beneath the Roman region. *Contributions to Mineralogy and Petrology* **90**, 244–257.

Rogers, N. W., Hawkesworth, C. J. & Palacz, Z. A. (1992). Phlogopite in the generation of olivine-melilitites from Namaqualand, South Africa and implications for element fractionation processes in the upper mantle. *Lithos* **28**, 347–365.

Sablukov, S. M. (1984). The question of origin stages and age of the Onega Peninsula pipes. *Doklady Akademii Nauk SSSR* **277**, 168–170 (in Russian).

Sablukov, S. M. (1987). Some peculiarities of the internal structure of the kimberlitic pipes. *Moscow: TsNIGRI Proceeding* **218**, 37–41 (in Russian).

Sablukov, S. M. (1990). Petrochemical series of kimberlite rocks. *Proceedings of the USSR Academy of Sciences* **313**, 935–939 (in Russian).

Sablukova, L. I. (1995). Mantle nodules in kimberlite rocks of Arkhangelsk. *Extended Abstracts: 6th International Kimberlite Conference*. Novosibirsk: United Institute of Geology, Geophysics and Mineralogy, Siberian Branch of the Russian Academy of Sciences Novosibirsk, pp. 484–486.

Sablukova, L. I., Sablukov, S., Griffin, W. L., O'Reilly, S. Y., Ryan, C. G., Win, T. T. & Grib, V. (1995). Lithosphere evolution in the Arkhangelsk kimberlite province. *Extended Abstracts: 6th International Kimberlite Conference*. Novosibirsk: United Institute of Geology, Geophysics and Mineralogy, Siberian Branch of the Russian Academy of Sciences Novosibirsk, pp. 487–489.

Salop, L. I. (1982). *Geological Development of the Earth in the Precambrian*. St Petersburg: Nedra (in Russian).

Scott-Smith, B. H., Skinner, E. M. W. & Loney, P. E. (1989). The Kapamba lamproites of the Luangwa valley, Eastern Zambia. In: Ross, J. (ed.) *Proceedings of the 4th International Kimberlite Conference, Perth. Geological Society of Australia Special Publication* **14**, 189–205.

Shcheglov, A. D., Moskaleva, V. N., Markovskiy, B. A., Kolbantsev, L. R., Orlova, M. P. & Smolkin, V. F. (1993). *Magmatism and Metallogeny of Riftogenic Systems in the Eastern Baltic Shield*. St Petersburg: Nedra (in Russian).

Sinitsin, A. V. & Grib, V. P. (1995). Arkhangelsk kimberlite province: field guidebook. *6th International Kimberlite Conference*. Novosibirsk: United Institute of Geology, Geophysics and Mineralogy, Siberian Branch of the Russian Academy of Sciences Novosibirsk.

Sinitsin, A. V. & Kushev, V. G. (1968). The Devonian trap formation of the Timan–Kola region. *Doklady Akademii Nauk SSSR* **178**, 1168–1170 (in Russian).

Sinitsin, A. V., Grib, V. P., Ermolaeva, L. A., Stankovskiy, A. E. & Starostin, B. A. (1982). The Vendian activity of the north part of the Russian plate. *Doklady Akademii Nauk SSSR* **264**, 680–682 (in Russian).

Sinitsin, A. V., Dauev, Y. M. & Grib, V. P. (1992). Structural position and productivity of kimberlites in the Arkhangelsk region. *Geologiya i Geofizika* **10**, 74–83 (in Russian).

Sinitsin, A., Ermolaeva, L. & Grib, V. (1994). The Arkhangelsk diamond-kimberlite province—a recent discovery in the north of the east European platform. *Proceedings of the 5th International Kimberlite Conference, Araxa, Vol. 1*. Rio de Janeiro: Companhia de Pesquisa de Recursos Minerais, pp. 27–33.

Skinner, E. M. W., Mahotkin, I. L. & Grütter, H. S. (1998). 'Melilite' in kimberlites. *Extended Abstracts: 7th International Kimberlite Conference*. Cape Town: University of Cape Town, pp. 817–819.

Sleep, N. H. (1996). Lateral flow of hot plume material ponded at sublithospheric depths. *Journal of Geophysical Research* **101**, 28065–28083.

Sleep, N. H. (1997). Lateral flow and ponding of starting plume material. *Journal of Geophysical Research* **102**, 10001–10012.

Smith, C. B. (1983). Pb, Sr and Nd isotope evidence for sources of southern African Cretaceous kimberlites. *Nature* **304**, 51–54.

Smith, J. V., Breenesholtz, R. & Dawson, J. B. (1978). Chemistry of micas from kimberlites and xenoliths 1. Micaceous kimberlites. *Geochimica et Cosmochimica Acta* **42**, 959–971.

Sobolev, A. V., Sobolev, N. V., Smith, C. B. & Dubessy, J. (1989). Fluid and melt compositions in lamproites and kimberlites based on the study of inclusions in olivine. In: Ross, J. (ed.) *Proceedings of the 4th International Kimberlite Conference, Perth. Geological Society of Australia Special Publication* **14**, 220–240.

Sobolev, N. V., Yefimova, E. S., Reimers, L. F., Zakharchenko, O. D., Makhin, A. I. & Usova, L. V. (1997). Mineral inclusions in diamonds of the Arkhangelsk kimberlite province. *Russian Geology and Geophysics* **38**, 379–393.

Stankovskiy, A. F., Verichev, E. M., Konstantinov, U. G., Scripnichenko, V. A. & Sobolev, V. K. (1977). The first occurrence of the effusive rocks within the Redkinskiy layers of the Vendian in the north of the Russian platform. *Doklady Akademii Nauk SSSR* **234**, 661–664 (in Russian).

Stankovskiy, A. F., Verichev, E. M., Grib, B. P., Scripnichenko, V. A. & Sobolev, V. K. (1979). The new type of magmatism within Vendian deposits in the north Russian platform. *Doklady Akademii Nauk SSSR* **247**, 1457–1460 (in Russian).

Staritskiy, U. G. (ed.) (1981). *History and Mineralisation of the Sedimentary Cover of the Russian Platform*. Leningrad: Nedra (in Russian).

Sun, S. S. & McDonough, W. F. (1989). Chemical and isotope systematics of oceanic basalts: implications for mantle compositions and processes. In: Saunders, A. D. & Norry, M. J. (eds) *Magmatism in the Ocean Basins*. Oxford: Blackwell, pp. 313–345.

Tainton, K. M. & McKenzie, D. (1994). The generation of kimberlites, lamproites and their source rocks. *Journal of Petrology* **35**, 787–817.

Thompson, R. N. & Gibson, S. A. (1991). Subcontinental mantle plumes, hot spots and pre-existing thinspots. *Journal of the Geological Society, London* **148**, 973–977.

Thompson, R. N., Morrison, M. A., Hendry, G. L. & Parry, S. J. (1984). An assessment of the relative roles of crust and mantle in magma genesis: an elemental approach. *Philosophical Transactions of the Royal Society of London, Series A* **310**, 549–590.

Thompson, R. N., Leat, P. T., Morrison, M. A., Hendry, G. L. & Gibson, S. A. (1990). Strongly potassic mafic magmas from lithospheric mantle sources during continental extension and heating: evidence from Miocene minettes of northwest Colorado, U.S.A. *Earth and Planetary Science Letters* **98**, 139–153.

Thompson, R. N., Gibson, S. A., Mitchell, J. G., Dickin, A. P., Leonardos, O. H., Brod, J. A. & Greenwood, J. C. (1998). Migrating Cretaceous–Eocene magmatism in the Serra do Mar alkaline province, SE Brazil: melts from the deflected Trindade mantle plume? *Journal of Petrology* **39**, 1493–1526.

Vartiainen, H. & Paarma, H. (1979). Geological characteristics of the Sokli carbonatite complex, Finland. *Economic Geology* **74**, 1296–1306.

Verichev, E. M., Sablukov, S. M., Sablukova, L. I. & Zhuravlev, D. Z. (1998). A new type of diamondiferous kimberlite of the Zimny Bereg area (pipe named after Vladimir Grib). *Extended Abstracts: 7th International Kimberlite Conference*. Cape Town: University of Cape Town, pp. 940–942.

Vollmer, R., Ogden, P. R., Schilling, J. G., Kingsley, R. H. & Waggoner, D. G. (1984). Nd and Sr isotopes in ultrapotassic volcanic rocks from the Leucite Hills, Wyoming. *Contributions to Mineralogy and Petrology* **87**, 359–368.

Watson, S. & McKenzie, D. (1991). Melt generation by plumes: a study of Hawaiian volcanism. *Journal of Petrology* **32**, 501–537.

White, R. S. & McKenzie, D. (1995). Mantle plumes and flood basalts. *Journal of Geophysical Research* **100**, 17543–17585.

Wilson, M. & Lyashkevich, Z. M. (1996). Magmatism and the geodynamics of rifting of the Pripyat–Dnieper–Donets rift, East European platform. *Tectonophysics* **268**, 65–81.

Woolley, A. R., Bergman, S. C., Edgar, A. D., Le Bas, M. J., Mitchell, R. H., Rock, N. M. S. & Scott-Smith, B. H. (1996). Classification of lamprophyres, kimberlites, and the kalsilitic, melilitic and leucitic rocks. *Canadian Mineralogist* **34**, 175–186.

Zaitsev, A. & Bell, K. (1995). Sr and Nd isotope data of apatite, calcite and dolomite as indicators of source, and the relationships of phoscorites and carbonatites from the Kovdor massif, Kola peninsula, Russia. *Contributions to Mineralogy and Petrology* **121**, 324–335.

Zhuravlev, D. Z., Chernyshev, I. V., Agapova, A. A. & Serduk, N. I. (1983). Precision isotopic analyses of neodymium in igneous rocks. *Izvestia Akademii Nauk SSSR* **12**, 23–40 (in Russian).

APPENDIX: ANALYTICAL METHODS

Electron microprobe analyses were obtained from polished-thin sections with a Cambridge Stereoscan S4-10 system with Kevex-7000 analyser operated at 15 kV and 0·02–0·03 mA sample current and Nick-wave correction program. Microprobe work was carried out in the Mineralogy–Petrography Institute, Freiburg University (Germany).

All of the samples were crushed in jaw-crusher and powdered in a corundum disc mill. Analyses of major elements in samples from the Zimniy Bereg pipes were

determined by wet chemistry at the Institute of Ore Deposits (IGEM, Moscow). In the same samples Li, Rb, Cs, Sr, Ba, Ni, Co, Cr and V concentrations were determined by atomic absorption and Zr, Nb, Y concentrations were determined by X-ray fluorescence (XRF) at IGEM (Moscow). Analyses of the major and trace elements of the Onega pipe samples were determined on fused discs and pressed powder pellets by XRF techniques at the Freiburg University (Germany). Hf, Sc, Ta, Th, U, REE were determined by instrumental neutron activation analysis (INAA) at IGEM (Moscow). Those samples in Table 6 with complete REE and other trace element data were analysed by inductively coupled plasma mass spectrometry (ICP-MS) at the University of Durham. Sample preparation techniques have been discussed by Thompson *et al.* (1998).

Sr and Nd isotopes were analysed on a Finnigan-MAT-262 mass-spectrometer, at IGEM (e.g. Zhuravlev *et al.*, 1983). Sr and Nd isotopic ratios were determined on the freshest massive whole-rock samples and separated autoliths from the Zimniy Bereg pipes and on clinopyroxene mineral separates from the Onega Peninsula pipes to avoid the effects of crustal contamination. The mean of $^{87}Sr/^{86}Sr$ ratios obtained for the E&A Sr standard is 0·708027 ($n = 7$) with 2σ SD of the mean of 0·000025. The mean of $^{143}Nd/^{144}Nd$ ratios made on the La Jolla Nd standard is 0·511843 ($n = 7$) with 2σ SD of the mean of 0·000016.